

1 **Dimitrios Stampoulis**

2 I am still not satisfied with the literature review the authors have conducted, as on the one hand
3 one citation (one of the authors' recently published article) is repeatedly used in many cases,
4 while on the other hand I believe that the authors can do a better job further enhancing their
5 literature review. Nevertheless, all of my previous concerns have been adequately addressed
6 by the authors, and the paper should now be acceptable for publication, following minor
7 revision, focusing on the aforementioned comment and the minor corrections indicated below:

8 **Accept, we have made an adjustment and only cited previous work when necessary and
9 use other references in other cases. Additional references have been included to support
10 the literature review.**

11 Technical Corrections-

12 1) Line 30 remove "the" after "Of these,"

13 **Accept**

14 2) Line 33 same after "Instead," and after "baseflow."

15 **Accept**

16 3) Line 43 The length of dry cycles is likely to

17 **Accept**

18 4) Lines 54-56 Awkward sentence; please rephrase

19 **Accept, as per reviewer 2 comments**

20 5) Lines 88, 89 "set up" and not "setup"

21 **Accept**

22 6) Line 157 remove “the” before “Krom Antonies” – the authors need to make sure that this
23 will be done for all similar cases throughout the text

24 **Accept, changes made throughout the paper**

25 7) Line 167 I do not have expertise in the relative field, but perhaps MG could be defined here

26 **Accept, MG defined line 146**

27 8) Line 557 remove “on”

28 **Accept**

29 9) Line 674 modeling

30 **Reject: In South Africa its modelling.**

31

32 **Anonymous**

33

34 The authors have modified the J2000 model to understand the contributions of the different
35 flow components to the Verlorenvlei lake, South Africa from the various contributing
36 tributaries. Overall, the study presents a significant body of work which adds to the available
37 literature in this area. Furthermore, the work is of value to South African hydrology, where
38 studies such of this that determine groundwater contributions together with surface water
39 contributions are rare.

40 The manuscript in the revised form, is well written, the methodology clear and the conclusions
41 generally supported by the findings. The authors have to a large extent addressed the comments

42 of the previous reviewers and significantly improved the paper. The figures and tables that have
43 been included in the revised version have improved the clarity of the paper.

44 It is my opinion that the paper still only touches on the ecological reserve aspects. The paper
45 is a sound contribution to modelling and the determination of the components of flow, by
46 attempting to relate to the ecological reserve the authors have detracted from the work as they
47 have not adequately addressed it.

48 **Noted, in the online peer review, concerns were made by an anonymous reviewer**
49 **regarding the ecological reserve, stating that the methodology followed was not inline**
50 **with South African ecological reserve assessments. Subsequently in the revisions we**
51 **withdrew some of the initial discussion points and conclusions, so that the revised version**
52 **is both inline with South African ecological reserve assessments as well as relating the**
53 **work presented to the need for better estimates to ensure sustainable water usage.**

54

55 The authors have used MODFLOW to validate the recharge estimates for the J2000 model
56 (Section 3.7.3; figure 7). Models should not be validated against each other, at most their
57 outputs can be compared. I would encourage the authors to use another dataset for the
58 calibration and validation, or to better document the pitfalls and uncertainties introduced with
59 this approach and why it was the only one possible.

60 **Accept, this was also a concern for reviewer 1 in the original paper, but we have included**
61 **additional references to validate the procedure.**

62 “This was done by aligning the MODFLOW recharge estimates and previous studies (Conrad
63 et al., 2004; Miller et al., 2017; Vegter, 1999; Weaver et al., 1999; Wu, 2005) with those of the

64 J2000, through adjustment of aquifer hydraulic conductivity from the MODFLOW
65 groundwater model of Krom Antonies (Watson, 2018) (Fig. 5)".

66 **"Recharge estimates from previous studies of the primary aquifer indicate recharge rates**
67 **of 0.2-3.4 % (Conrad et al., 2004), and 8% (Vegter, 1999), while for the TMG aquifer 13**
68 **% (Wu, 2005), 27% (Miller et al., 2017) and 17.4 % (Weaver and Talma, 2005) of MAP."**

69

70 The flows (Figure 9) from all tributaries are significantly higher during the last wet period
71 (2007 – 2017). Please note that the average rainfall values used in the text and those in added
72 in Figure 9 are not the same and should be corrected. The findings show higher flows in the
73 latter period that are far greater than what would be anticipated from the higher rainfall. A 30
74 mm change in rainfall resulted in a more than doubling of the average baseflow response. It is
75 during the latter period that the authors state that irrigation in the catchment has been expanding
76 and that there is this growing threat of agriculture expansion to the water resources, but this
77 has not been accounted for in the model. Have the authors considered the cause of the marked
78 higher streamflow response – is it a change in the nature of the rainfall distribution in the latter
79 period, a change in the timing of the rainfall?

80 **Accept, this is absolutely true. We looked into the model results for the first wet cycle and**
81 **the second, and saw a marked increase in soil moisture, with a minor decrease in potential**
82 **ET. Looking into the standard deviation between yearly rainfall for the first wet cycle,**
83 **the dry cycle and the second wet cycle there is more than a doubling in the yearly rainfall**
84 **variability, which is the result of this high flow variability in the second wet cycle. We**
85 **have incorporated the STD for the three cycles in the text and a small sentence in the**
86 **discussion about this, as the paper length has got quite long.**

87

88 “The estimated flow exceedance probabilities indicated that during the 2008-2017 wet cycle
89 average lake inflows exceeded the average evaporation demand, **although yearly rainfall is**
90 **twice as variable in comparison to the first wet cycle between 1987-1996**”. **Line 35-38**

91 “This is particularly evident in the measured water level data from station G3T001, where
92 measured water levels have a large daily standard deviation (0.62) (Watson et al., 2018). **The**
93 **daily inflows of water into the Verlorenvlei has also been subject to significant rainfall**
94 **variability, with yearly rainfall between the first wet cycle (1987-1996) being twice as**
95 **variable in comparison to the second wet cycle (2007-2017). The change in rainfall**
96 **variability has had a significant impact on soil moisture conditions, resulting in not only**
97 **larger peak discharges but also lengthened low flow conditions.** With climate change likely
98 to impact the length and severity of dry cycles, it is likely that the lake will dry up more
99 frequently into the future, which could have severe implications on the biodiversity that relies
100 on the lake’s habitat for survival. Of importance to the lake’s survival is the protection of river
101 inflows during wet cycles, where the lake requires these inflows for regeneration”. **Line 649-**
102 **659**

103 The modelling results showed that on average the streamflow influxes were not able to meet
104 the evaporation demand of the lake, **with yearly rainfall becoming more variable.** **Line 689-**
105 **691**

106

107 Specific comments:

108 Introduction, Pg 3, Line 54/55 – insert “were” between “problems thought”

109 **Accept, as per reviewer 1 request**

110 Caption Fig 1. Isohyets spelt incorrectly

111 **Accept**

112 Section 2, Pg 8, Line 153 – The sentence “Where rainfall was less than 50 % of the MAP
113 (1965-1969 and 2015-2017), concerns over the amount of streamflow required to support the
114 lake have been raised.” Consider rephrasing this sentence. I would presume that the concerns
115 mentioned are now for the recent past not the 1960’s. You have stated that agric expansion has
116 been a more recent phenomena in the catchment and is probably a driver of the concerns.

117 **Accept**, “Recently, where rainfall was less than 50 % of the MAP (2015-2017), concerns over
118 the amount of streamflow required to support the lake have been raised”

119 Table 2, what are the units of AVE?

120 **Noted, absolute sum of differences between measured and simulated**, “absolute volume
121 error (AVE)”

122

123 **Distributive rainfall/runoff modelling to understand runoff to baseflow**
124 **proportioning and its impact on the determination of reserve requirements**
125 **of the Verlorenvlei estuarine lake, west coast, South Africa**

126

127 Andrew Watson¹, Jodie Miller¹, Manfred Fink², Sven Kralisch^{2,3}, Melanie Fleischer², and
128 Willem de *Clercq*³*Clercq*⁴

129 1. *Department of Earth Sciences, Stellenbosch University, Private Bag X1, Matieland 7602,*
130 *South Africa*

131 2. *Department of Geoinformatics, Friedrich-Schiller-University Jena, Loebdergraben 32,*
132 *07743 Jena, Germany*

133 3. *German Aerospace Center (DLR), Institute of Data Science, Maelzerstraße 3, 07745 Jena,*
134 *Germany*

135 4. *Stellenbosch Water Institute, Stellenbosch University, Private Bag X1, Matieland, 7602,*
136 *South Africa*

137

138 **Keywords:** rainfall/runoff modelling, Verlorenvlei reserve, J2000

139 **Abstract**

140 River systems that support high biodiversity profiles are conservation priorities world-wide.
141 Understanding river eco-system thresholds to low flow conditions is important for the
142 conservation of these systems. While climatic variations are likely to impact the streamflow
143 variability of many river courses into the future, understanding specific river flow dynamics
144 with regard to streamflow variability and aquifer baseflow contributions are central to the
145 implementation of protection strategies. While streamflow is a measurable quantity, baseflow
146 has to be estimated or calculated through the incorporation of hydrogeological variables. In

147 this study, the groundwater components within the J2000 rainfall/runoff model were distributed
148 to provide daily baseflow and streamflow estimates needed for reserve determination. The
149 modelling approach was applied to the RAMSAR-listed Verlorenvlei estuarine lake system on
150 the west coast of South Africa which is under threat due to agricultural expansion and climatic
151 fluctuations. The sub-catchment consists of four main tributaries, ~~the~~-Krom Antonies, Hol,
152 Bergvallei and Kruismans. Of these, ~~the~~-Krom Antonies was initially presumed the largest
153 baseflow contributor, but was shown to have significant streamflow variability, attributed to
154 the highly conductive nature of the Table Mountain Group sandstones and quaternary
155 sediments. Instead, ~~the~~-Bergvallei was identified as the major contributor of baseflow. ~~The~~ Hol
156 was the least susceptible to streamflow fluctuations due to the higher baseflow proportion (56
157 %), as well as the dominance of less conductive Malmesbury shales that underlie it. The
158 estimated flow exceedance probabilities indicated that during the 2008-2017 wet cycle average
159 lake inflows exceeded the average evaporation demand, although yearly rainfall is twice as
160 variable in comparison to the first wet cycle between 1987-1996. During the 1997-2007 dry
161 cycle, average lake inflows are exceeded 85~~–~~% of the time by the evaporation demand. The
162 exceedance probabilities estimated here suggest that inflows from the four main tributaries are
163 not enough to support Verlorenvlei, with the evaporation demand of the entire lake being met
164 only 35~~–~~% of the time. This highlights the importance of low occurrence events for filling up
165 Verlorenvlei, allowing for regeneration of lake-supported ecosystems. As climate change
166 drives increased temperatures and rainfall variability, the length of dry cycles ~~are-is~~ likely to
167 increase into the future and result in the lake drying up more frequently. For this reason, it is
168 important to ensure that water resources are not overallocated during wet cycles, hindering
169 ecosystem regeneration and prolonging the length of these dry cycle conditions.

170 **1. Introduction**

171 Functioning river systems offer numerous economic and social benefits to society including
172 water supply, nutrient cycling and disturbance regulation amongst others (Costanza et al., 1997;
173 Nelson et al., 2009; Postel and Carpenter, 1997)(Nelson et al., 2009; Postel and Carpenter,
174 1997). As a result, many countries worldwide have endeavoured to protect river ecosystems,
175 although only after provision has been made for basic human needs (Gleick, 2003; Richter et
176 al., 2012; Ridoutt and Pfister, 2010). However, the implementation of river protection has been
177 problematic, because many river courses and flow regimes have been severely altered due to
178 socio-economic development (Gleeson and Richter, 2018; O'Keeffe, 2009; Richter, 2010).
179 River health problems were thought to only result from low-flow conditions and if minimum
180 flows were kept above a critical level, the river's ecosystem would be protected (Poff et al.,
181 1997; Tennant, 1976). It is now recognised that a more natural flow regime, which includes
182 floods as well as low and medium flow conditions, is required for sufficient ecosystem
183 functioning (Arthington et al., 2018; Bunn and Arthington, 2002; Olden and Naiman, 2010;
184 Postel and Richter, 2012). For these reasons, before protection strategies can be developed or
185 implemented for a river system, a comprehensive understanding of the river flow regime
186 dynamics is necessary.

187 River flow regime dynamics include consideration of not just the surface water in the river but
188 also other water contributions including runoff, interflow and baseflow which are all essential
189 for the maintenance of the discharge requirements. Taken together these factors all contribute
190 to the hydrological components of what is called the ecological reserve, the minimum
191 environmental conditions needed to maintain the ecological health of a river system (Hughes,
192 2001; King and Louw, 1998; Richter et al., 2003). A variety of different methods have been
193 developed to incorporate various river health factors into ecological reserve determination
194 (Acreman and Dunbar, 2004; Bragg et al., 2005). One of the simplest and most widely applied,

Formatted: Not Highlight

Field Code Changed

Commented [AW1]:

195 is where compensation flows are set below reservoirs and weirs, using flow duration curves to
196 derive mean flow or flow exceedance probabilities (e.g. Harman and Stewardson, 2005). This
197 approach focusses purely on hydrological indices, which are rarely ecologically valid (e.g.
198 Barker and Kirmond, 1998; **Lancaster and Downes, 2010**).

199 More comprehensive ecological reserve estimates such as functional analysis are focused on
200 the whole ecosystem, including both hydraulic and ecological data (e.g. ELOHA: Poff et al.,
201 2010; Building Block Methodology: King and Louw, 1998). While these methods consider that
202 a variety of low, medium and high flow events are important for maintaining ecosystem
203 diversity, they require specific data regarding the hydrology and ecology of a river system,
204 which in many cases does not exist, has not been recorded continuously or for sufficient
205 duration (Acreman and Dunbar, 2004; **Richter et al., 2012**). To speed up ecological reserve
206 determination, river flow records have been used to analyse natural seasonality and variability
207 of flows (e.g. Hughes and Hannart, 2003). However, this approach requires long-term
208 streamflow and baseflow timeseries. Whilst streamflow is a measurable quantity subject to a
209 gauging station being in place, baseflow has to be modelled based on hydrological and
210 hydrogeological variables.

211 Rainfall/runoff models can be used to calculate hydrological variables using distributive
212 surface water components (e.g. J2000: Krause, 2001; **SWAT: Arnold et al., 1998**) but the
213 groundwater components are generally lumped within conventional modelling frameworks. In
214 contrast, groundwater models, which distribute groundwater variables (e.g. MODFLOW:
215 Harbaugh et al., 2000; **FEFLOW: Diersch, 2002**) are frequently set up to lump climate
216 components. In order to accurately model daily baseflow, which is needed for reserve
217 determination, modelling systems need to be setup such that both groundwater and climate
218 variables are treated in a **distributive distributed** manner (e.g Bauer et al., 2006; Kim et al.,
219 2008). Rainfall/runoff models, which use Hydrological Response Units (HRUs) as an entity of

220 homogenous climate, rainfall, soil and landuse properties (Flügel, 1995; Leavesley and
221 Stannard, 1990), are able to reproduce hydrographs through model calibration (Wagener and
222 Wheater, 2006; Young, 2006). However, they are rarely able to correctly proportion runoff and
223 baseflow components (e.g. Willems, 2009; Hughes, 2004). To correctly determine
224 groundwater baseflow using rainfall/runoff models such as the J2000, aquifer components need
225 to be distributed. This can be achieved using net recharge and hydraulic conductivity collected
226 through aquifer testing or groundwater modelling.

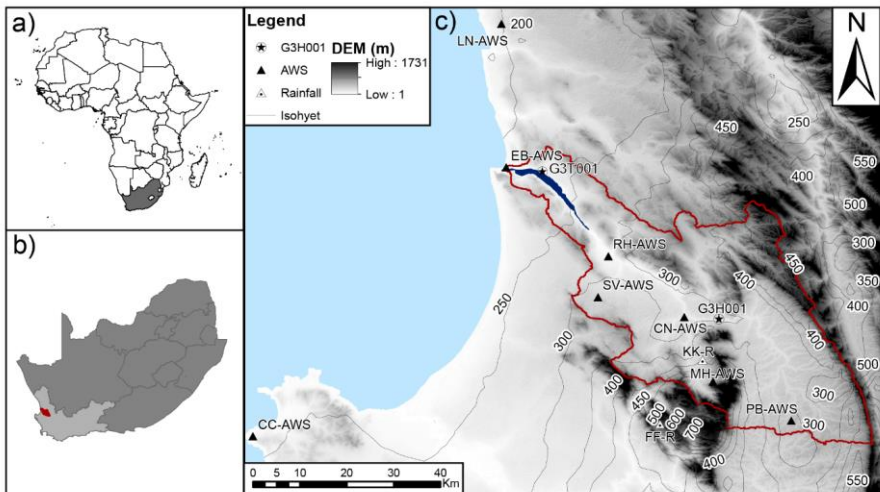
227 To better understand river flow variability, a rainfall/runoff model was distributed to
228 incorporate aquifer hydraulic conductivity within model HRUs using calibrated values from a
229 MODFLOW groundwater model (Watson, 2018). The model was setup for the RAMSAR
230 listed Verlorenvlei estuarine lake on the west coast of South Africa, which is under threat from
231 climate change, agricultural expansion and mining exploration. The rainfall/runoff model used
232 was J2000 as this model had previously been set up in the region and model variables were
233 well established (e.g Bugan, 2014; Schulz et al., 2013). While the estuarine lake's importance
234 is well documented (Martens et al., 1996; Wishart, 2000), the lake's reserve is not well
235 understood, due to the lack of streamflow and baseflow estimates for the main feeding
236 tributaries of the system. The modelling framework developed in this study aimed to
237 understand the flow variability of the lake's feeding tributaries, to provide the hydrological
238 components (baseflow and runoff proportioning) of the tributaries needed to understand the
239 lake reserve. The surface water and groundwater components of the model were calibrated for
240 two different tributaries which were believed to be the main source of runoff and baseflow for
241 the sub-catchment. The baseflow and runoff rates calculated from the model indicate not only
242 that the lake system cannot be sustained by baseflow during low flow periods but also that the
243 initial understanding of which tributaries are key to the sustainability of the lake system was
244 not correct. The results have important implications for how we understand water dynamics in

245 water stressed catchments and the sustainability of ecological systems in these types of
246 environments generally.

247 **2. Study site**

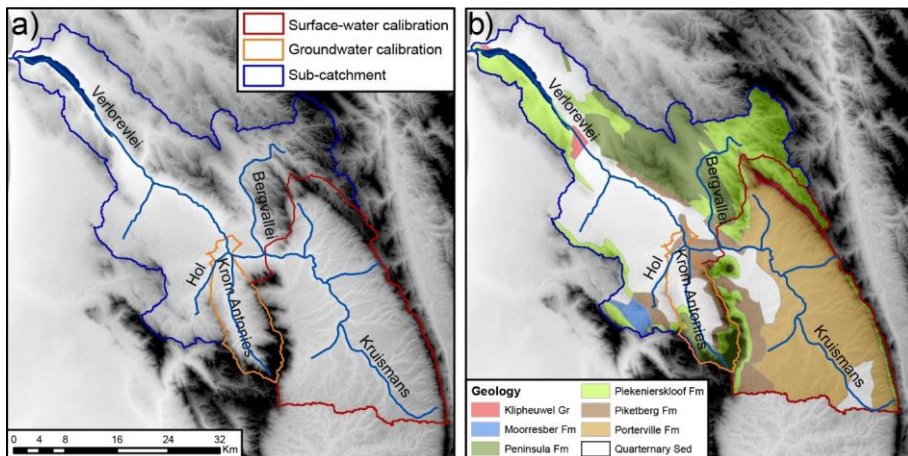
248 Verlorenvlei is an estuarine lake situated on the west coast of South Africa, approximately 150
249 km north of the metropolitan city of Cape Town (Fig. 1). The west coast, which is situated in
250 the Western Cape Province of South Africa, is subject to a Mediterranean climate where the
251 majority of rainfall is received between May to September. The Verlorenvlei lake, which is
252 approximately 15 km² in size draining a watershed of 1832 km², forms the southern sub-
253 catchment of the Olifants/Doorn water management area (WMA). The lake hosts both Karroid
254 and Fynbos biomes, with a variety of vegetation types (e.g Arid Estuarine Saltmarsh, Cape
255 Inland Salt pans) sensitive to reduced inflows of freshwater (Helme, 2007). A sandbar created
256 around a sandstone outcrop (Table Mountain Group: [TMG](#)) allows for an intermittent
257 connection between salt and fresh water. During storms or extremely high tides, water scours
258 the sand bar allowing for a tidal exchange, with a constant inflow of salt water continuing until
259 the inflow velocity decreases enough for a new sand bar to form (Sinclair et al., 1986).

260 The lake is supplied by four main tributaries which are ~~the~~ Krom Antonies, Bergvallei, Hol and
261 Kruismans (Fig. 2). The main freshwater sources are presumed to be ~~the~~ Krom Antonies and
262 ~~the~~ Bergvallei, which drain the mountainous regions to the south (Piketberg) and north of the
263 sub-catchment respectfully ([Sigidi, 2018](#)). ~~The~~ Hol and Kruismans tributaries are variably
264 saline ([Sigidi, 2018](#)) ([Sigidi, 2018](#)), due to high evaporation rates in the valley. Average daily
265 temperatures during summer within the sub-catchment are between 20-30 °C, with estimated
266 potential evaporation rates of 4 to 6 mm.d⁻¹ (Muche et al., 2018). In comparison, winter daily
267 average temperatures are between 12-20 °C, with estimated potential evaporation rates of 1 to
268 3 mm.d⁻¹ (Muche et al., 2018).



269

270 Figure 1: a) Location of South Africa, b) the location of the study catchment within the Western
 271 Cape and c) the extend of the Verlorenvlei sub-catchment with the climate stations, gauging
 272 station (G3H001), measured lake water level (G3T001) and rainfall isohyets

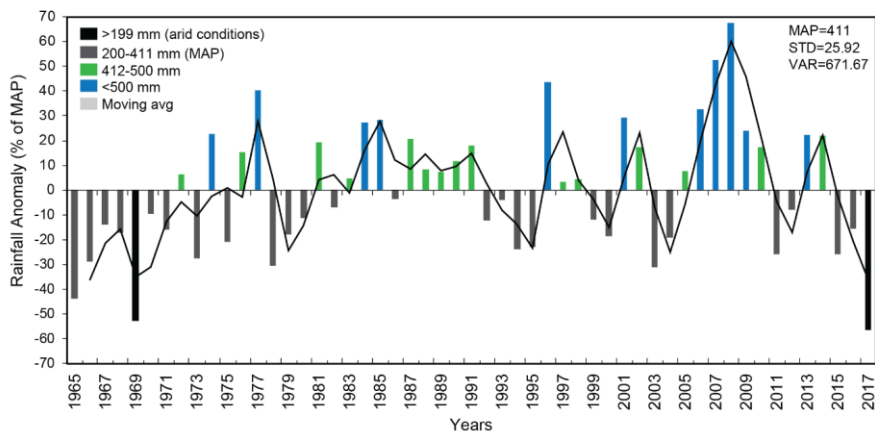


273

274 Figure 2: a) The Verlorenvlei sub-catchment with the surface water calibration tributary
 275 (Kruismans) and groundwater calibration tributary (Krom Antonies) and b) the hydrogeology
 276 of the sub-catchment with Malmesbury shale formations (MG: Klipheuwel, Mooresberg,
 Peninsula Fm)

277 Porterville, Piketberg), Table Mountain Group formations (Peninsula, Piekenierskloof) and
278 quaternary sediments

279 Rainfall for the sub-catchment, recorded over the past 52 years by local farmers at KK-R (Fig.
280 1) shows large yearly variability (26 %) between the Mean Annual Precipitation (MAP ~~200-411~~
281 mm) and measured rainfall (Fig. 3). Where rainfall was greater than 500 mm.yr^{-1} (2006-2010),
282 it is presumed that the lake is supported by a constant influx of streamflow from the feeding
283 tributaries. ~~Recently, where~~ rainfall was less than 50 % of the MAP (~~1965-1969 and~~ 2015-
284 2017), concerns over the amount of streamflow required to support the lake have been raised.



285

286 Figure 3: The difference between MAP and measured rainfall (plotted as rainfall anomaly) for
287 52 years (1965-2017) at location KK-R in the valley of ~~the~~ Krom Antonies (after Watson *et*
288 *al.*, 2018).

289 While rainfall varies greatly between years in the sub-catchment, it is also spatially impacted
290 by elevational differences. The catchment valley which receives the least MAP $100-350 \text{ mm.yr}^{-1}$
291 ¹ (Lynch, 2004), is between 0-350 masl and is comprised of quaternary sediments that vary in
292 texture, although the majority of the sediments in the sub-catchment are sandy in nature. The

293 higher relief mountainous regions of the sub-catchment between 400-1300 masl receive the
294 highest MAP 400-800 mm.yr⁻¹ (Lynch, 2004), are mainly comprised of fractured TMG
295 sandstones, (youngest to oldest): Peninsula, Graafwater (not shown), and Piekernerskloof
296 formations (Fig. 2) (Johnson et al., 2006). Underlying the sandstones and quaternary sediments
297 are the MG shales, which are comprised of the Mooresberg, Piketberg and Klipheuwel
298 formations (Fig. 2) (Rozendaal and Gresse, 1994). Agriculture is the dominant water user in
299 the sub-catchment with an estimated usage of 20[–]% of the total recharge (DWAF, 2003;
300 Watson, 2018) (Conrad et al., 2004; DWAF, 2003), with the main food crop being potatoes.
301 The MG shales and quaternary sediments, which host the secondary and primary aquifer
302 respectfully, are frequently used to supplement irrigation during the summer months of the
303 year. During winter, the majority of the irrigation water needed for crop growth is supplied by
304 the sub-catchment tributaries or the lake itself. The impact of irrigation on the lake is still
305 regarded as minimal (Meinhardt et al., 2018) but further investigation is still required for future
306 investigation. For additional information regarding the study site refer to Watson *et al.*, (2018)
307 and (Conrad *et al.*, (2004)).

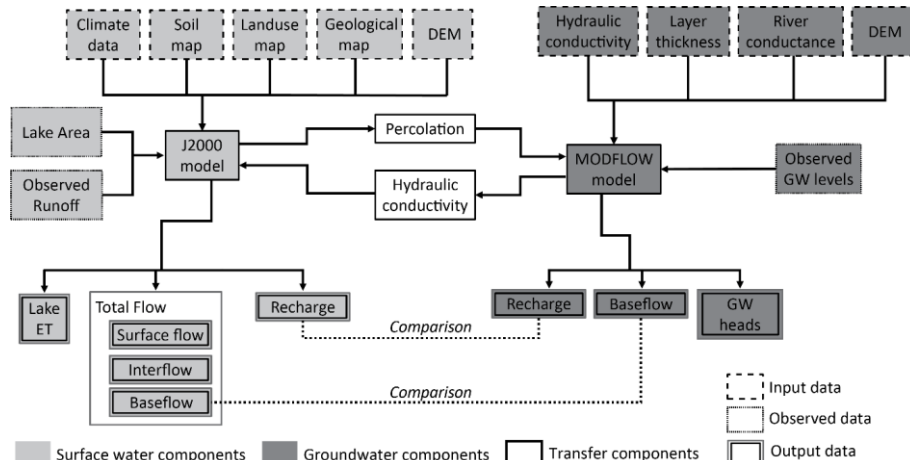
Formatted: Font: Italic

308 3. Methodology

309 In this study, the J2000 coding was adapted to incorporate distributive distributed groundwater
310 components for the model HRU's (Fig. 4). This was done by aligning the MODFLOW recharge
311 estimates and previous studies (Conrad et al., 2004; Miller et al., 2017; Vetger, 1995; Weaver
312 and Talma, 2005; Wu, 2005) estimates with those of the J2000, through adjustment of aquifer
313 hydraulic conductivity from the MODFLOW groundwater model of the Krom Antonies
314 (Watson, 2018) (Fig. 5). The assigned hydraulic conductivity for each geological formation
315 was thereafter transferred across the entire J2000 model of the sub-catchment. The adaption
316 applied to the groundwater components influenced the proportioning of water routed to runoff

317 and baseflow within the J2000 model. To validate the outputs of the model, an empirical mode
318 decomposition (EMD) (Huang et al., 1998) was applied to compute the proportion of variation
319 in discharge timeseries that attributed to a high and low water level change at the sub-catchment
320 outlet. The streamflow estimates were thereafter compared with the lake evaporation demand,
321 to understand the sub-catchment water balance.

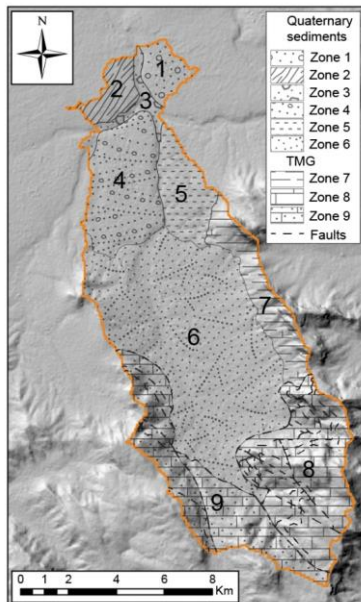
322 The J2000 model incorporated ~~distributive-distributed~~ climate, soil, landuse and
323 hydrogeological information, with aquifer hydraulic conductivity transferred from
324 MODFLOW as described above (Fig. 4). The measured streamflow was used to both calibrate
325 and validate the model, with the landuse dataset being selected according to the period of
326 measured streamflow. Changes in the recorded lake level were used alongside remote sensing
327 to estimate the lake evaporation rate. The impact of irrigation was not included in the model,
328 as there is not enough information available regarding agricultural water use. This is currently
329 one of the major limitations with the study approach presented here and will be the focus of
330 future work. The HRU delineation, model regionalisation, water balance calculations, lateral
331 and reach routing as well as the lake evaporation procedure are presented. Thereafter the input
332 data for the model, the calibration and validation procedures as well as the EMD protocol used,
333 is described.



334 Surface water components Groundwater components Transfer components

335 Figure 4: Schematic of the model structure, showing the processors simulated by the J2000 and

336 MODFLOW and the components that were transferred from the MODFLOW model



337

338 Figure 5: The aquifer hydraulic zones used for the groundwater calibration of the J2000 (after

339 Watson, 2018)

340 **3.1 Hydrological Response Unit Delineation**

341 HRUs and stream segments (reaches) are used within the J2000 model for distributedive
342 topographic and physiological modelling. In this study, the HRU delineation made use of a
343 digital elevation model, with slope, aspect, solar radiation index, mass balance index and
344 topographic wetness being derived. Before the delineation process, gaps within the digital
345 elevation model were filled using a standard fill algorithm from ArcInfo (Jenson and
346 Domingue, 1988). The AML (ArcMarkupLanguage) automated tool (Pfennig et al., 2009) was
347 used for the HRU delineation, with between 13 and 14 HRUs/km² being defined
348 (Pfannschmidt, 2008). After the delineation of HRUs, dominant soil, land use and geology
349 properties were assigned to each. The hydrological topology was defined for each HRU by
350 identifying the adjacent HRUs or stream segments that received water fluxes.

351 **3.2 Model regionalisation**

352 Rainfall and relative humidity are the two main parameters that are regionalised within the
353 J2000 model. While a direct regionalisation using an inverse-distance method (IDW) and the
354 elevation of each HRU can be applied to rainfall data, the regionalisation of relative humidity
355 requires the calculation of absolute humidity. The regionalisation of rainfall records was
356 applied by defining the number of weather station records available and estimating the
357 influence on the rainfall amount for each HRU. A weighting for each station using the distance
358 of each station to the area of interest was applied to each rainfall record, using an elevation
359 correction factor (Krause, 2001). The relative humidity and air temperature measured at set
360 weather stations were-was used to calculate the absolute humidity. Absolute humidity was
361 thereafter regionalised using the IDW method, station and HRU elevation. After the
362 regionalisation had been applied, the absolute humidity was converted back to relative
363 humidity through calculation of saturated vapor pressure and the maximum humidity.

364 **3.3 Water balance calculations**

365 The J2000 model is divided into calculations that impact surface water and groundwater
366 processors. The J2000 model distributes the regionalised precipitation (P) calculated for each
367 HRU using a water balance defined as:

$$P = R + Int_{max} + ETR + \Delta Soil_{sat} \quad (1)$$

368 where R is runoff (mm) (RD1 - surface runoff; RD2 - interflow), Int_{max} is vegetation canopy
369 interception (mm), ETR is 'real' evapotranspiration and $\Delta Soil_{sat}$ is change in soil saturation.
370 The surface water processes have an impact on the amount of modelled runoff and interflow,
371 while the groundwater processors influence the upper and lower groundwater flow
372 components.

373 **3.3.1 Surface water components**

374 Potential evaporation (ETP) within the J2000 model is calculated using the Penman Monteith
375 equation. Before evaporation was calculated for each HRU, interception was subtracted from
376 precipitation using the leaf area index and leaf storage capacity for vegetation (a_rain)
377 (Supplementary: Table 1). Evaporation within the model considers several variables that
378 influence the overall modelled evaporation. Firstly, evaporation is influenced by a slope factor,
379 which was used to reduce ETP based on a linear function. Secondly, the model assumed that
380 vegetation transpires until a particular soil moisture content where ETP is reached, after which
381 modelled evaporation was reduced proportionally to the ETP, until it became zero at the
382 permanent wilting point.

383 The soil module in the J2000 model is divided up into processing and storage units. Processing
384 units in the soil module include soil-water infiltration and evapotranspiration, while storage
385 units include middle pore storage (MPS), large pore storage (LPS) and depression storage. The
386 infiltrated precipitation was calculated using the relative saturation of the soil, and its maximum

387 infiltration rate (SoilMaxInfSummer and SoilMaxInfWinter) (Supplementary: Table 1).
 388 Surface runoff was generated when the maximum infiltration threshold was exceeded. The
 389 amount of water leaving LPS, which can contribute to recharge, was dependant on soil
 390 saturation and the filling of LPS via infiltrated precipitation. Net recharge (R_{net}) was estimated
 391 using the hydraulic conductivity ($SoilMaxPerc$), the outflow from LPS (LPS_{out}) and the slope
 392 (*slope*) of the HRU according to:

$$R_{net} = LPS_{out} \times (1 - \tan(slope) \cdot SoilMaxPerc) \quad (2)$$

393 The hydraulic conductivity, $SoilMaxPerc$ and the adjusted LPS_{out} were thereafter used to
 394 calculate interflow (IT_f) according to:

$$IT_f = LPS_{out} \times (\tan(slope) \cdot SoilMaxPerc) \quad (3)$$

395 with the interflow calculated representing the sub-surface runoff component RD2 and is routed
 396 as runoff within the model.

397 3.3.2 Groundwater components

398 The J2000 model for the Verlorenvlei sub-catchment was set up with two different geological
 399 reservoirs: (1) the primary aquifer (upper groundwater reservoir - RG1), which consists of
 400 quaternary sediments with a high permeability; and (2) the secondary aquifer (lower
 401 groundwater reservoir- RG2), made up of MG shales and TMG sandstones (Table 1).

Aquifer	Formation	Type	RG1_max	RG2_max	RG1_k	RG2_k	RG1_active	Kf_geo	depthRG1
		Sediments	(mm)	(mm)	(d)	(d)	(n/a)	(mm/d)	(cm)
Primary	Quaternary Sediments	Sediments	50	700	100	431	1	500	1750
Secondary/MG	Moorresberg Formation	Shale Greywacke	0	580	0	350	0	950	1750
Secondary/MG	Porterville Formation	Shale Greywacke	0	560	0	335	0	2	1750
Secondary/MG	Piketberg Formation	Shale Greywacke	0	1000	0	600	0	950	1750
Secondary/MG	Klipheuwel Group	Shale Greywacke	0	500	0	300	0	950	1750
Secondary/TMG	Peninsula Formation	Sandstone	0	1000	0	600	0	950	1750
Secondary/TMG	Piekenierskloof Formation	Sandstone	0	600	0	400	0	1	1750

402
 403 Table 1: The J2000 hydrogeological parameters RG1_max, RG2_max, RG1_k, RG2_Kf_geo
 404 and depthRG1 assigned to the primary and secondary aquifer formations for the Verlorenvlei
 405 sub-catchment

406 The model therefore considered two baseflow components, a fast one from ~~the~~-RG1 and a
 407 slower one from RG2. The filling of the groundwater reservoirs was done by net recharge, with
 408 emptying of the reservoirs possible by lateral subterranean runoff as well as capillary action in
 409 the unsaturated zone. Each groundwater reservoir was parameterised separately using the
 410 maximum storage capacity (maxRG1 and maxRG2) and the retention coefficients for each
 411 reservoir (*recRG1* and *recRG2*). The outflow from the reservoirs was determined as a function
 412 of the actual filling (*actRG1* and *actRG2*) of the reservoirs and a linear drain function.
 413 Calibration parameters *recRG1* and *recRG2* are storage residence time parameters. The
 414 outflow from each reservoir was defined as:

$$OutRG1 = \frac{1}{gwRG1Fact \times recRG1} \times actRG1 \quad (4)$$

$$OutRG2 = \frac{1}{gwRG2Fact \times recRG2} \times actRG2 \quad (5)$$

415 where- *OutRG1* is the outflow from the upper reservoir, *OutRG2* is the outflow from the lower
 416 reservoir and *gwRG1Fact* / *gwRG2Fact* are calibration parameters for the upper and lower
 417 reservoir used to determine the outflow from each reservoir. To allocate the quantity of net
 418 recharge between the upper (RG1) and lower (RG2) groundwater reservoirs, a calibration
 419 coefficient *gwRG1RG2sdist* was used to distribute the net recharge for each HRU using the
 420 HRU slope. The influx of groundwater into the shallow reservoir (*inRG1*) was defined as:

$$inRG1 = R_{net} \times (1 - (1 - \tan(slope))) \times gwRG1RG2sdist \quad (6)$$

421 The influx of net recharge into the lower groundwater reservoir (*inRG2*) was defined as:

$$inRG2 = R_{net} \times (1 - \tan(slope)) \times gwRG1RG2sdist \quad (7)$$

422 with the combination of *OutRG1* and *OutRG2* representing the baseflow component that is
 423 routed as an outflow from the model.

424 **3.4 Lateral and reach routing**

425 Lateral routing was responsible for water transfer within the model and included HRU influxes
426 and discharge through routing of cascading HRUs from the upper catchment to the exit stream.
427 HRUs were either able to drain into multiple receiving HRUs or into reach segments, where
428 the topographic ID within the HRU dataset determined the drain order. The reach routing
429 module was used to determine the flow within the channels of the river using the kinematic
430 wave equation and calculations of flow according to Manning and Strickler. The river
431 discharge was determined using the roughness coefficient of the stream (Manning roughness),
432 the slope and width of the river channel and calculations of flow velocity and hydraulic radius
433 calculated during model simulations.

434 **3.5 Calculations of lake evaporation rate**

435 The lake evaporation rate was based on the ETP calculated by the J2000 and an estimated lake
436 surface area. The lake was modelled as a unique HRU (water as the land-cover type), with a
437 variable area which was estimated using remote sensing data from Landsat 8 and Sentinel-2
438 and the measured lake water level at G3T001 (Fig. 1). To infill lake surface area when remote
439 sensing data was not available, a relationship was created between the estimated lake's surface
440 area and the measured water level between 2015-2017. Where lake water level data was not
441 available (before 1999), an average long-term monthly value was used for the lake evaporation
442 calculations.

443 **3.6 J2000 Input data**

444 **3.6.1 Surface water parameters**

445 Climate and rainfall: Rainfall, windspeed, relative humidity, solar radiation and air temperature
446 were monitored by Automated Weather Stations (AWS) within and outside of the study
447 catchment (Fig. 1). Of the climate and rainfall data used during the surface water modelling

448 (Watson et al., 2018), data was sourced from seven AWS's of which four stations were owned
449 by the South African Weather Service (SAWS) and three by the Agricultural Research Council
450 (ARC). Two stations that were installed for the surface water modelling, namely Moutonshoek
451 (M-AWS) and Confluence (CN-AWS) were used for climate and rainfall validation due to their
452 short record length. Additional rainfall data collected by farmers at high elevation at location
453 FF-R and within the middle of the catchment at KK-R were used to improve the climate and
454 rainfall network density.

455 Landuse classification: The vegetation and landuse dataset that was used for the sub-catchment
456 (CSIR, 2009) included five different landuse classes: 1) wetlands and waterbodies, 2)
457 cultivated (temporary, commercial, dryland), 3) shrubland and low fynbos, 4) thicket,
458 bushveld, bush clumps and high fynbos and 5) cultivated (permanent, commercial, irrigated).
459 Each different landuse class was assigned an albedo, root depth and seal grade value based on
460 previous studies (Steudel et al., 2015)(Supplementary: Table 2). The Leaf Area Index (LAI)
461 and vegetation height varies by growing season with different values of each for the particular
462 growing season. While surface resistance of the landuse varied monthly within the model, the
463 values only vary significantly between growing seasons.

464 Soil dataset: The Harmonized World Soil Database (HWSD) v1.2 (Batjes et al., 2012) was the
465 input soil dataset, with nine different soil forms within the sub-catchment (Supplementary:
466 Table 3). Within the HWSD, soil depth, soil texture and granulometry were used to calculate
467 and assign soil parameters within the J2000 model. MPS and LPS which differ in terms of the
468 soil structure and pore size were determined in Watson et al. (2018), using pedotransfer
469 functions within the HYDRUS model (Supplementary: Table 3).

470 Streamflow and water levels: Streamflow, measured at the Department of Water Affairs
471 (DWA) gauging station G3H001 between 1970-2009, at the outlet of the Kruismans tributary

472 (Het Kruis) (Fig 1 and 3), was used for surface water calibration. The G3H001 two-stage weir
473 could record a maximum flow rate of $3.68 \text{ m}^2 \cdot \text{s}^{-1}$ due to the capacity limitations of the structure.
474 After 2009, the G3H001 structure was decommissioned due to structural damage, although
475 repairs are expected in the near future due to increasing concerns regarding the influx of
476 freshwater into the lake. Water levels measured at the sub-catchment outlet at DWA station
477 G3T001 (Fig 1) between 1994 to 2018 were used for EMD filtering.

478 **3.6.2 Groundwater parameters**

479 Net recharge and hydraulic conductivity: The hydraulic conductivity values used for the
480 groundwater component adaptation were collected from detailed MODFLOW modelling of ~~the~~
481 Krom Antonies tributary (Fig. 5) (Watson, 2018). The net recharge and aquifer hydraulic
482 conductivity for ~~the~~ Krom Antonies tributary, was estimated through PEST autocalibration
483 using hydraulic conductivities from previous studies (SRK, 2009; UMVOTO-SRK, 2000) and
484 potential recharge estimates (Watson et al., 2018).

485 Hydrogeology: Within the hydrogeological dataset, parameters assigned include maximum
486 storage capacity (RG1 and RG2), storage coefficients (RG1 and RG2), the minimum
487 permeability/maximum percolation (Kf_geo of RG1 and RG2) and depth of the upper
488 groundwater reservoir (depthRG1). The maximum storage capacity was determined using an
489 average thickness of each aquifer and the total number of voids and cavities, where the primary
490 aquifer thickness was assumed to be between 15-20 m (Conrad et al., 2004), and the secondary
491 aquifer between 80-200 m (SRK, 2009). The maximum percolation of the different geological
492 formations was assigned hydraulic conductivities using the groundwater model for ~~the~~ Krom
493 Antonies sub-catchment (Watson, 2018). The J2000 geological formations were assigned
494 conductivities to modify the maximum percolation value to ensure internal consistency with
495 recharge values calculated using MODFLOW (Table 1).

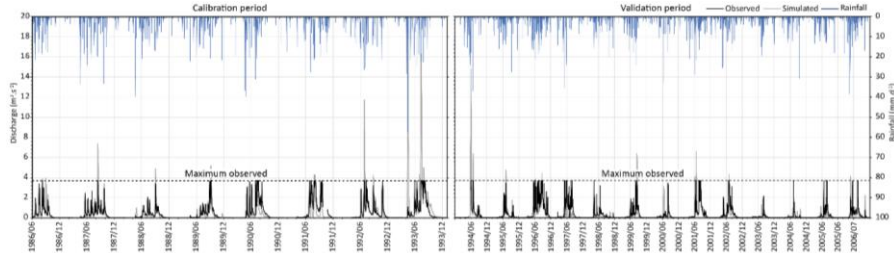
496 **3.7 J2000 model calibration**

497 **3.7.1 Model sensitivity**

498 The J2000 sensitivity analysis for Verlorenvlei sub-catchment was presented in Watson *et al.*,
499 (2018) and therefore only a short summary is presented here. In this study, parameters that
500 were used to control the ratio of interflow to percolation were adjusted, which in the J2000
501 model include a slope (SoilLatVertDist) and max percolation value. The sensitivity analysis
502 conducted by Watson *et al.*, (2018) showed that for high flow conditions (E2) (Nash-Sutcliffe
503 efficiency in its standard squared), model outputs are most sensitive to the slope factor, while
504 for low flow conditions (E1) (modified Nash-Sutcliffe efficiency in a linear form) the model
505 outputs were most sensitive to the maximum infiltration rate of the soil (ie. the parameter
506 maxInfiltrationWet) (Supplementary: Figure 1). The max percolation was moderately sensitive
507 during wet and dry conditions, and together with the slope factor, controlled the interflow to
508 percolation portioning proportioning that was calibrated in this study.

509 **3.7.2 Surface water calibration**

510 The surface water parameters of the model were calibrated for ~~the~~ Kruismans tributary (688
511 km²) (Fig. 3) using the gauging data from G3H001 (Fig. 6 and Table 1). The streamflow data
512 used for the calibration was between 1986-1993, with model validation between 1994 to 2007
513 (Fig. 6). This specific calibration period was selected due to the wide range of different runoff
514 conditions experienced at the station, with both low and high flow events being recorded. For
515 the calibration, the modelled discharge was manipulated in the same fashion, with a DT limit
516 (discharge table) of 3.68 m³/s, so that the tributary streamflow behaved as measured discharge.



517
 518 Figure 6: The surface water calibration (1986-1993) and validation (1994-2006) of the J2000
 519 model using gauging data from the G3H001

520 An automated model calibration was performed using the “Nondominating Sorting Genetic
 521 Algorithm II” (NSGA-II) multi-objective optimisation method (Deb et al., 2002) with 102⁴³
 522 model runs being performed. Narrow ranges of calibration parameters (FC_Adaptation,
 523 AC_Adaptation, soilMAXDPS, gwRG1Fact and gwRG2Fact) were chosen to (1) ensure that
 524 the modelled recharge from J2000 was within an order of magnitude of recharge from the
 525 MODFLOW model and previous studies; (2) ~~to~~ achieve a representative sub-catchment
 526 hydrograph. As objective functions, Nash-Sutcliffe-Efficiency based on absolute differences
 527 (E1) and squared differences 2 (E2) as well as the E2, E1 and the average bias in % (Pbias)
 528 were utilized for the calibration (Krause et al., 2005) (Table 2). The choice of the optimized
 529 parameter set was made to ensure that E2 was better than 0.57 (best value was 0.57) and the
 530 Pbias better than 5% (Table 1). From the automated calibration, 308 parameter sets were
 531 determined with the best E1 being chosen to ensure that the model is representative of low flow
 532 conditions (Table 1).

533 **3.7.3 Model validation**

534 Observed vs modelled streamflow: For the surface water model validation, the streamflow
 535 records between 1994-2007 were used, where Nash-Sutcliffe-Efficiency (E1 and E2) absolute
 536 values (E1) and squared differences (E2) of the Nash-Sutcliffe efficiency were reported. The

537 Pbias was also used as an objective function to report the model performance by comparison
 538 between measured and modelled streamflow (Table 2). Although gauging station limitations
 539 resulted in good objective functions from the model, the performance of objective functions
 540 E1, E2, Pbias reduced between the validation and calibration period (Table 2). During the
 541 calibration period there was a good fit between modelled and measured streamflow (Pbias=-
 542 1.82), with a significant difference between modelled and measured streamflow during the
 543 validation period (Pbias=-19.2). The calibration was performed over a wet cycle (1986-1997),
 544 which resulted in a more common occurrence of streamflow events that exceeded $3.68 \text{ m}^3 \cdot \text{s}^{-1}$,
 545 thereby reducing the number of calibration points. In contrast the validation was performed
 546 over a dry cycle (1997-2007), which resulted in more data points as few streamflow events
 547 exceeded $3.68 \text{ m}^3 \cdot \text{s}^{-1}$.

	Calibration 1987-1993	Validation 1994-2007
E1	0.55	0.53
E2	0.57	0.56
LogE1	0.28	0.10
LogE2	0.46	0.19
AVE	-19.24	-269.20
R ²	0.62	0.58
Pbias	-1.82	-19.23758
KGE	0.79	0.67417

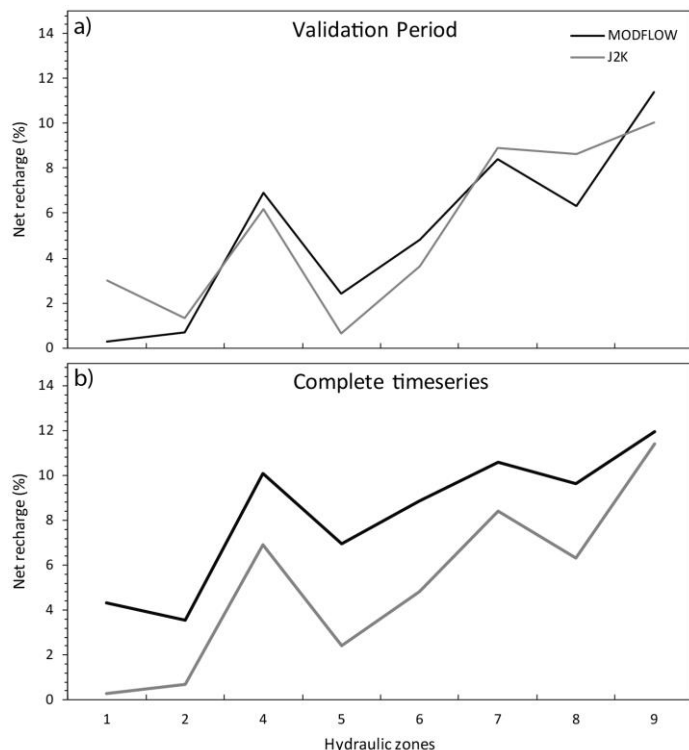
548

549 Table 2: Value of ~~T~~he objective functions E1, E2, logarithmic versions of E1 and E2, absolute
 550 volume average error (AV~~E~~E), coefficient of determination (R^2), Pbias and Kling Gupta
 551 Efficiency (KGE) (Gupta et al., 2009) ~~used~~ for ~~the~~ surface water calibration (1987-1993) and
 552 validation (1994-2007)

Formatted: Superscript

553 The J2000 and MODFLOW recharge estimates: With adjustment of hydraulic conductivities
 554 from MODFLOW to J2000 it was possible to converge the net recharge estimates between 1.~~5~~3
 555 % with a range of recharge of 0.65-10.03.~~5~~ % for the J2000 and 0.3-11.40.~~5~~ % for MODFLOW.
 556 Recharge estimates from previous studies of the primary aquifer indicate recharge rates of 0.2-

557 3.4 % (Conrad et al., 2004), and 8 % Vetger, 1995, while for the TMG aquifer 13 % (Wu,
 558 2005, 27 % (Miller et al., 2017) and 17.4 % (Weaver and Talma, 2005) of MAP. J2000
 559 estimates had an average value of 5.30 –% while MODFLOW was 5.20 –% for the eight
 560 hydraulic zones of the Krom Antonies. The coefficient of determination (R^2) between net
 561 recharge from the J2000 and MODFLOW was 0.81. Across the entire dataset J2000
 562 overestimated groundwater recharge by 2.75 –% relative to MODFLOW, although the
 563 coefficient of determination produced an R^2 of 0.92 which is better than during the validation
 564 period.

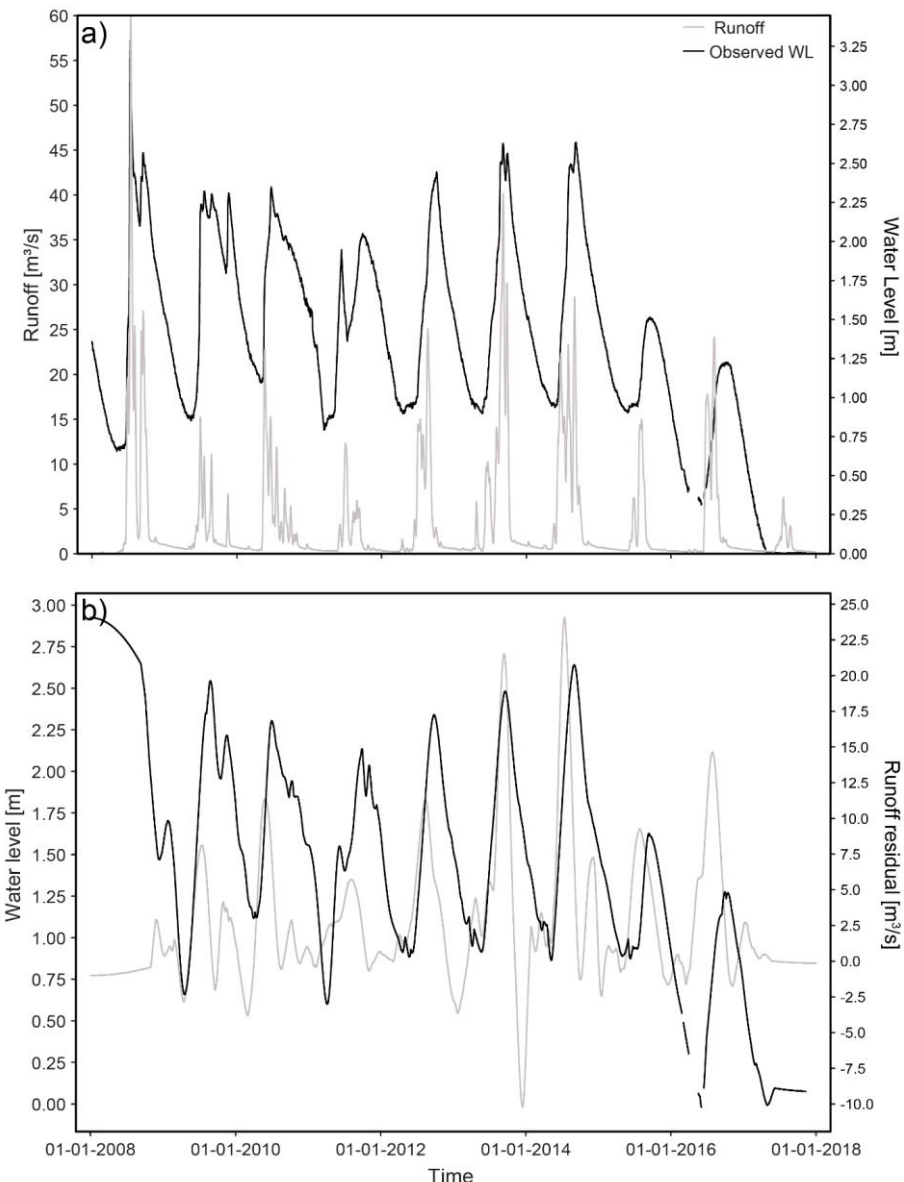


565

566 Figure 7: The groundwater calibration for each hydraulic zone with a) net recharge for the
567 J2000 and MODFLOW during the model calibration (2016) and b) the net recharge deviation
568 between MODFLOW and J2000 across the entire modelling timestep (1986-2017)

569 **3.8 EMD filtering**

570 To account for missing streamflow data between 2007-2017, an Empirical Mode
571 Decomposition (EMD) (Huang et al., 1998) was applied to the measured water level data at
572 the sub-catchment outlet (G3T001)(Fig. 1) between 1994 to 2018 (Fig 8a). EMD is a method
573 for the decomposition of nonlinear and nonstationary signals into sub-signals of varying
574 frequency, so-called intrinsic mode functions (IMF), and a residuum signal. By removing one
575 or more IMF or the residuum signal, certain frequencies (e.g. noise) or an underlying trend can
576 be removed from the original time series data. This approach was successfully applied to the
577 analysis of river runoff data (Huang et al., 2009) and forecasting of hydrological time series
578 (Kisi et al., 2014). In this study, EMD filtering was used to remove high frequency sub-signals
579 from simulated runoff and measured water level data to compare the more general seasonal
580 variations of both signals (Fig. 8b).



581

582 Figure 8: a) The water level fluctuations at station G3T001 with modelled runoff and b) the
 583 EMD filtering showing the variation in discharge timeseries attributed a water level change at
 584 the station

585 **4. Results**

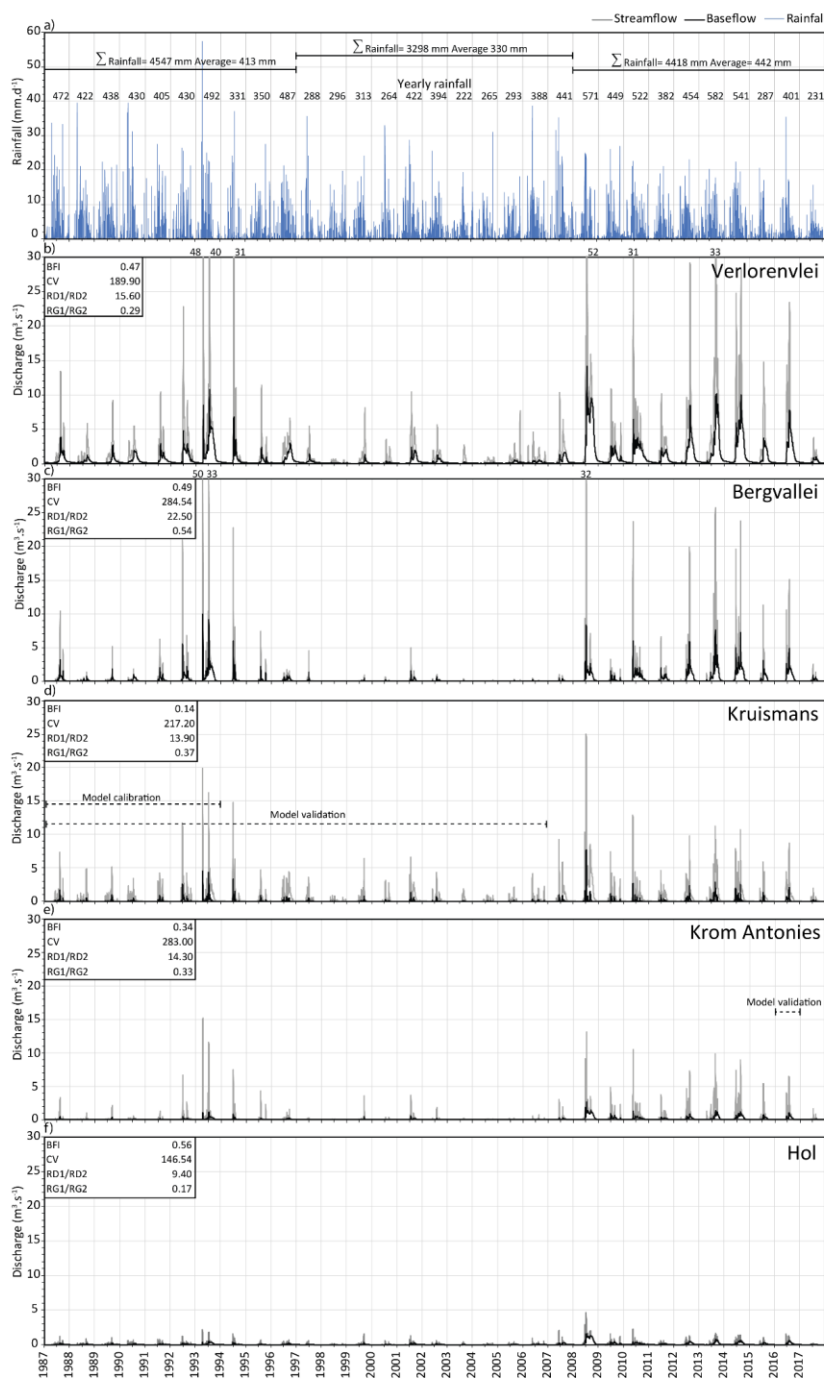
586 The J2000 model was used to simulate both runoff and baseflow, with runoff being comprised
587 of direct surface runoff (RD1) and interflow (RD2) and baseflow simulated from the primary
588 (RG1) and secondary aquifer (RG2). Below, the results of the modelled streamflow and
589 baseflow are presented, along with the total flow contribution of each tributary, the runoff to
590 baseflow proportioning and stream exceedance probabilities. The coefficient of variation (CV)
591 was used to determine the streamflow variability of each tributary, while the baseflow index
592 (BFI) was used to determine the baseflow and runoff proportion.

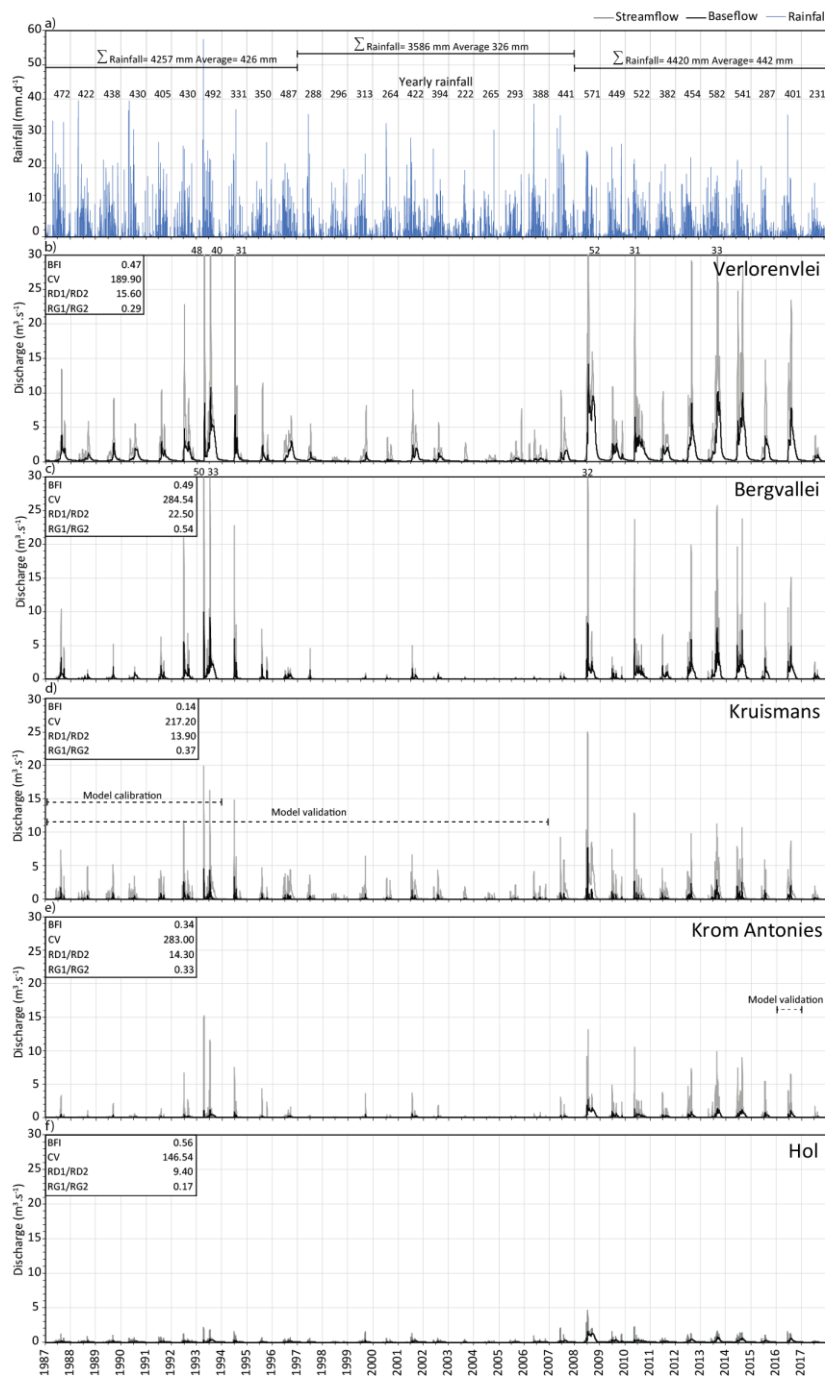
593 **4.1 Streamflow and baseflow**

594 Streamflow for the sub-catchment shows two distinctively wet periods (1987-~~1997-1996~~ and
595 ~~2007-2008~~-2017), separated by a dry period (~~1997-1997~~-200~~77~~) (Fig. 9). Yearly sub-catchment
596 rainfall volumes between 1987-~~1997-1996~~ were between 288 and 492 mm/yr⁻¹, with an average
597 of ~~404-426~~ mm.yr⁻¹ and standard deviation (STD) of 51 mm.yr⁻¹. For this period, average yearly
598 streamflow ~~between~~ was 1.4 m³.s⁻¹, with an average baseflow contribution of 0.63 m³.s⁻¹. The
599 modelled streamflow reached a maximum of 48 m³.s⁻¹ in 1993, where 5 m³.s⁻¹ of baseflow was
600 generated after 58 mm of rainfall was received. Between 199~~77~~-2007 (dry period) sub-
601 catchment yearly rainfall was between 222 and 394 mm/yr⁻¹ with an average of ~~330-326~~ mm.yr⁻¹
602 and STD of 69 mm.yr⁻¹ (Fig. 9). For this same period, average yearly streamflow was 0.44
603 m³.s⁻¹, with an average baseflow contribution of 0.18 m³.s⁻¹. The modelled streamflow reached
604 a maximum of 11 m³.s⁻¹ in 2002, with a baseflow contribution of 2.5 m³.s⁻¹ after 28 mm of
605 rainfall was received. During the second wet period between ~~2007-2008~~-2017 sub-catchment
606 yearly rainfall was between 231 and 582 mm.yr⁻¹ with an average of ~~427-442~~ mm.yr⁻¹ and STD
607 of 112 mm.yr⁻¹ (Fig. 9). Over this same period, average yearly streamflow was 2.5 m³.s⁻¹ with
608 an average baseflow contribution of 1.3 m³.s⁻¹. The modelled streamflow reached a maximum

609 of $52 \text{ m}^3 \cdot \text{s}^{-1}$ in 2008, with $13 \text{ m}^3 \cdot \text{s}^{-1}$ of baseflow generated after two consecutive rainfall events

610 each of 25 mm.

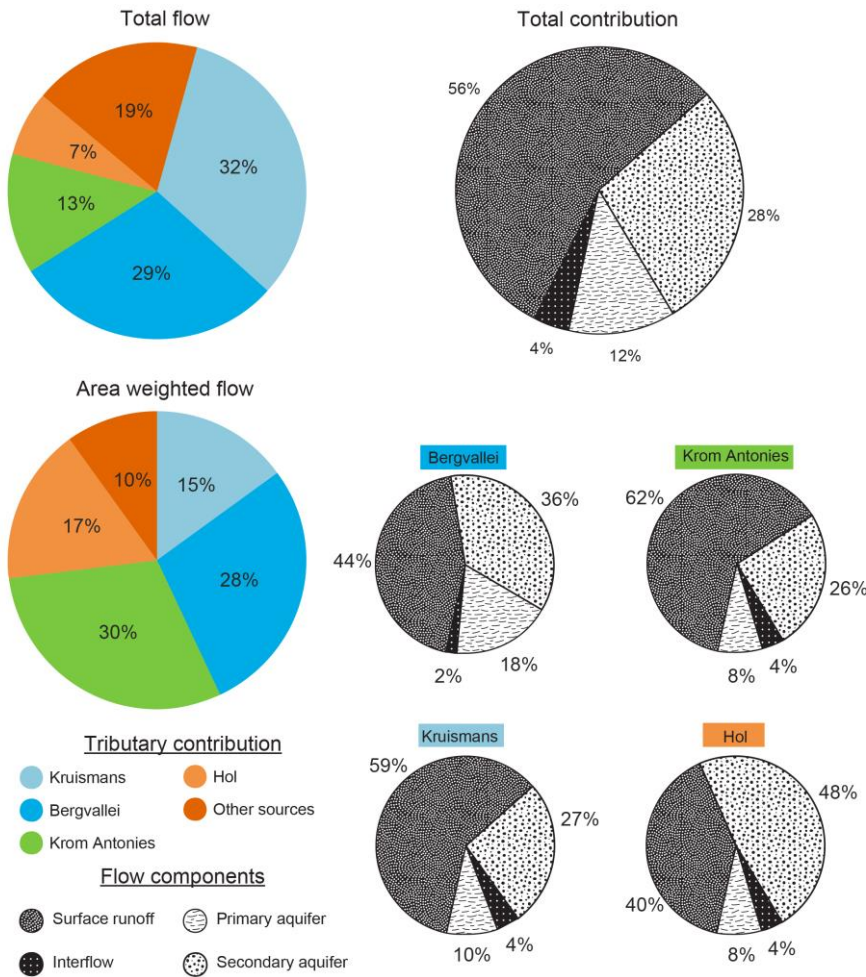




613 Figure 9: a) Average sub-catchment rainfall between 1987-2017 showing wet cycles (1987-
614 1997 and 2008-2017), Modelled streamflow and baseflow inflows
615 for the b) Verlorenvlei, c) Bergvallei, d) Kruismans, e) Krom Antonies and f) Hol tributaries
616 with estimated BFI, CV, RD1/RD2, RG1/RG2

617 **4.2 Tributary contributions**

618 The four main feeding tributaries (Bergvallei, Kruismans, Hol and Krom Antonies) together
619 contribute 81% of streamflow for the Verlorenvlei, with the additional 19% from small
620 tributaries near Redelinghuys (Fig. 10). The Kruismans contributes most of the total
621 streamflow at 32%, but only 15% of the area-weighted contribution as its sub-catchment is
622 the largest of the four tributaries at 688 km² (Fig. 10). The Bergvallei with a sub-catchment of
623 320 km², contributes 29% of the total flow with an area weighted contribution of 28%. The
624 Krom Antonies has the largest area weighted contribution of 30% due to its small size (140
625 km²) in comparison to the other tributaries, although the Krom Antonies contributes only 13%
626 of the total flow (Fig. 10). The Hol sub-catchment at 126 km² makes up the smallest
627 contribution to the total flow of only 7%, but has a weighted contribution of 17% (Fig. 10).



628

629 Figure 10: The Verlorenvlei reserve flow contributions (total flow and area weighted flow) of
 630 ~~the~~ Kruismans, Bergvallei, Krom Antonies and Hol as well as flow component separation
 631 into surface runoff (RD1), interflow (RD2), primary aquifer flow (RG1) and secondary
 632 aquifer flow (RG2).

633 **4.3 Flow variability**

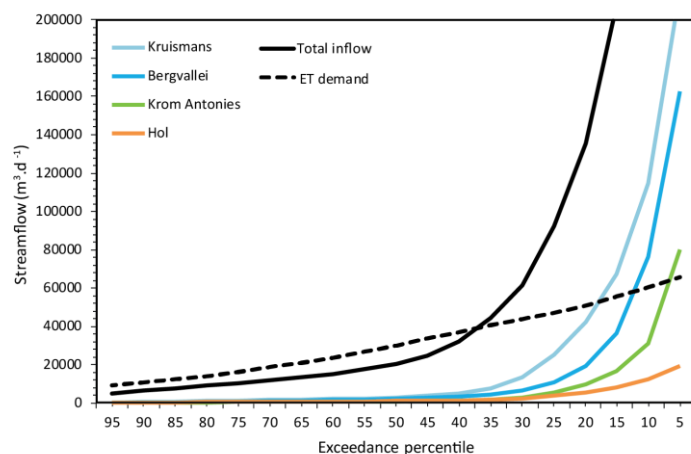
634 Streamflow that enters Verlorenvlei has a large daily variability with a coefficient of variation
635 (CV) of 189.90 (Fig. 9). This is mainly due to high streamflow variability from ~~the~~-Kruismans
636 (32₊%) with a CV of 217.20, which is the major total flow contributor (Fig 10). ~~The~~-Bergvallei
637 and Krom Antonies, which both have high streamflow variability with CV values of 284.54
638 and 283.00 respectfully (Fig. 9), further contribute to the high variability of streamflow that
639 enters the lake. While ~~the~~-Hol reduces the overall streamflow variability with a CV of 146.54,
640 it is a minor total flow contributor (7₊%) and therefore does not reduce the overall streamflow
641 variability significantly (Fig. 10).

642 Streamflow that enters Verlorenvlei is dominated by surface runoff which makes up 56₊% of
643 total flow, with groundwater and interflow contributing 40₊% and 4₊% respectfully (Fig. 10).
644 The large surface runoff dominance in streamflow entering the lake, is due to a high surface
645 runoff contribution from ~~the~~-Kruismans and Krom Antonies, which contribute 26₊% of total
646 flow from surface runoff. However, for ~~the~~-Bergvallei and Hol, surface runoff contributions
647 are less dominant with 16₊% of the total, while the total groundwater contribution is 20₊%
648 from these tributaries. Across all four tributaries, the secondary aquifer is the dominant
649 baseflow component with 28₊% of total flow, with the primary aquifer contributing 12₊%. ~~The~~
650 Bergvallei and Kruismans contribute the majority of primary aquifer baseflow with 8₊% of the
651 total. The secondary aquifer baseflow is mainly contributed by ~~the~~-Kruismans and Bergvallei,
652 where together 18₊% of the total is received. Interflow across the four tributaries is uniformly
653 distributed with 0.3 – 1₊% of the total flow being contributed from each tributary.

654 **4.4 Flow exceedance probabilities**

655 The flow exceedance probability, which is a measure of how often a given flow is equalled or
656 exceeded was calculated for each of the tributaries as well as the lake water body. The results

657 for the flow exceedance probabilities includes flow volumes which are exceeded 95 %, 75 %,
 658 50 %, 25 % and 5 % of the time. The 95 percentile corresponds to a lake inflow of $0.054 \text{ m}^3 \cdot \text{s}^{-1}$
 659 or $4,702 \text{ m}^3 \cdot \text{d}^{-1}$, with between 0.001 - $0.004 \text{ m}^3 \cdot \text{s}^{-1}$ from the feeding tributaries (Fig. 11 and
 660 Table 3). The 75-percentile flow, which is exceeded 3/4 of the time corresponds to an inflow
 661 of $0.119 \text{ m}^3 \cdot \text{s}^{-1}$ or $10,303 \text{ m}^3 \cdot \text{d}^{-1}$, with between 0.005 - $0.015 \text{ m}^3 \cdot \text{s}^{-1}$ from the feeding tributaries.
 662 Average (50 percentile) streamflow flowing into the Verlorenvlei is $0.237 \text{ m}^3 \cdot \text{s}^{-1}$ or $20,498$
 663 $\text{m}^3 \cdot \text{d}^{-1}$, with between 0.010 - $0.035 \text{ m}^3 \cdot \text{s}^{-1}$ from the feeding tributaries. The 25-percentile flow,
 664 which is exceeded $\frac{1}{4}$ of the time corresponds to a lake inflow of $1,067 \text{ m}^3 \cdot \text{s}^{-1}$ or $92,204 \text{ m}^3 \cdot \text{d}^{-1}$
 665 with between 0.044 - $0.291 \text{ m}^3 \cdot \text{s}^{-1}$ from the feeding tributaries. The lake inflows that are
 666 exceeded 5 % of the time correspond to $6.939 \text{ m}^3 \cdot \text{s}^{-1}$ or $599,535 \text{ m}^3 \cdot \text{d}^{-1}$ with between 0.224 -
 667 $2.49 \text{ m}^3 \cdot \text{s}^{-1}$ from the feeding tributaries.



668

669 Figure 11: The streamflow exceedance percentiles and evaporation demand of the Verlorenvlei
 670 reserve, with the contributions from each feeding tributary

Exceedance percentile	Lake ET	Verlorenvlei		Kruismans		Bergvallei		Krom Antonies		Hol	
	$m^3.d^{-1}$	$m^3.s^{-1}$	$m^3.d^{-1}$	$m^3.s^{-1}$	$m^3.d^{-1}$	$m^3.s^{-1}$	$m^3.d^{-1}$	$m^3.s^{-1}$	$m^3.d^{-1}$	$m^3.s^{-1}$	$m^3.d^{-1}$
95	9158	0.054	4702	0.004	346	0.001	69	0.001	109	0.002	176
90	10956	0.074	6356	0.007	604	0.002	191	0.003	232	0.003	269
85	12559	0.088	7628	0.010	830	0.004	366	0.004	319	0.004	353
80	14249	0.104	8979	0.012	1072	0.007	596	0.005	392	0.005	434
75	16330	0.119	10303	0.015	1291	0.010	839	0.005	459	0.006	508
70	18653	0.136	11759	0.018	1517	0.013	1104	0.006	534	0.007	587
65	21152	0.155	13373	0.021	1791	0.016	1381	0.007	602	0.008	676
60	23791	0.176	15180	0.024	2104	0.019	1657	0.008	685	0.009	786
55	26979	0.203	17575	0.029	2506	0.023	1965	0.009	772	0.011	913
50	30057	0.237	20498	0.035	3032	0.027	2309	0.010	882	0.012	1058
45	33467	0.286	24669	0.043	3755	0.032	2807	0.012	1024	0.014	1222
40	36760	0.371	32023	0.058	5022	0.041	3511	0.015	1258	0.017	1439
35	40391	0.516	44598	0.089	7699	0.053	4613	0.020	1745	0.021	1790
30	43814	0.710	61310	0.156	13511	0.076	6599	0.033	2824	0.029	2481
25	47062	1.067	92204	0.291	25182	0.123	10619	0.062	5387	0.044	3814
20	50997	1.571	135726	0.489	42242	0.223	19295	0.110	9511	0.065	5655
15	55797	2.399	207275	0.780	67408	0.421	36354	0.192	16594	0.096	8262
10	60162	3.759	324746	1.324	114432	0.885	76477	0.359	31045	0.141	12191
5	65418	6.939	599535	2.490	215152	1.884	162795	0.929	80305	0.224	19312

671

672 Table 3: The streamflow exceedance percentiles and lake evaporation demand for the
 673 Verlorenvlei reserve, with the contributions from the Kruismans, Bergvallei, Krom Antonies
 674 and Hol ($m^3.s^{-1}$ and $m^3.d^{-1}$)

675 5. Discussion

676 The adaptation of the J2000 rainfall/runoff model was used to understand the flow
 677 contributions of the main feeding tributaries, the proportioning of baseflow to surface runoff
 678 as well as how often the inflows exceed the lake evaporation demand. Before a comparison
 679 with previous baseflow estimates can be made and the impact of evaporation on the lake
 680 reserves assessed, the model limitations and catchment flow dynamics must also be assessed.

681 5.1 Model limitations and performance

682 A major limitation facing the development and construction of comprehensive modelling
 683 systems in sub-Saharan Africa is the availability of appropriate climate and streamflow data.
 684 For this study, while there was access to over 20 years of streamflow records, the station was

685 only able to measure a maximum of $3.68 \text{ m}^3.\text{s}^{-1}$, which hindered calibration of the model for
686 high flow events. As such, the confidence in the model's ability to simulate high streamflow
687 events using climate records is limited. While the availability of measured data is a limitation
688 that could affect the modelled streamflow, discontinuous climate records also hindered the
689 estimations of long time series streamflow.

690 Over the course of the 3031-year modelling period, a number of climate stations used for
691 regionalisation were decommissioned and were replaced by stations in different areas. This
692 required adaption of climate regionalisation for simulations over the entire 3031-year period to
693 incorporate the measured streamflow from the gauging station. To account for missing
694 streamflow records since 2007, an EMD filtering protocol was applied to the runoff data (Fig.
695 6). The results from the EMD filtering showed that after removing the first nine IMFs, the local
696 maxima of both signals match the seasonal water level maxima during most of the years. While
697 considerable improvement can be made to the EMD filtering, the results show some agreement
698 which suggested that the simulated runoff was representative of inflows into the lake.

699 **5.2 Catchment dynamics**

700 Factors that impact on streamflow variability are important for understanding river flow regime
701 dynamics. Previously, factors that affected streamflow variability such as CV and BFI values
702 were used to determine how susceptible particular river systems were to drought (e.g Hughes
703 and Hannart, 2003). While CV values have been used to account for climatic impacts such as
704 dry and wet cycles, BFI values are associated with runoff generation processes that impact the
705 catchment. For most river systems, BFI values are generally below 1 implying that runoff
706 exceeds baseflow. In comparison CV values can be in excess of 10 implying high variability
707 in streamflow volumes (Hughes and Hannart, 2003). In this study, these two measurements

708 have been applied to tributaries as opposed to quaternary river systems, to understand the
709 streamflow input variability into the Verlorenvlei.

710 The highest proportion of streamflow needed to sustain the Verlorenvlei lake water level is
711 received from the Bergvallei tributary, although the area weighted contribution from ~~the~~ Krom
712 Antonies is more significant (Fig. 10). However, CV values for the Bergvallei indicate high
713 streamflow variability. This is partially due to the high surface runoff component in modelled
714 streamflow within the Bergvallei in comparison to the minor interflow contribution, suggesting
715 little sub-surface runoff. While streamflow from the Bergvallei tributary is 54% groundwater,
716 which would suggest a more sustained streamflow, due to the TMG dominance as well as a
717 high primary aquifer contribution, baseflow from the Bergvallei is driven by highly conductive
718 rock and sediment materials. Similarly, CV values for ~~the~~ Krom Antonies indicate high
719 streamflow variability due to the presence of a high baseflow contribution from the conductive
720 TMG and primary aquifers. Although ~~the~~ Krom Antonies has a larger interflow component,
721 which would reduce streamflow variability, the dominant TMG presence within this tributary
722 partially compensates for the subsurface flow contributions.

723 In contrast, ~~the~~ Hol has a much smaller daily streamflow variability in comparison to both ~~the~~
724 Bergvallei and ~~the~~ Krom Antonies (Fig. 9). While streamflow from ~~the~~ Hol tributary is mainly
725 comprised of baseflow (56%), the dominance of low conductive shale rock formations as well
726 as a large interflow component results in reduced streamflow variability. While the larger shale
727 dominance in this tributary not only results in a more sustained baseflow from the secondary
728 aquifer, it also results in a large interflow component due to the limited conductivity of the
729 shale formations. Compounding the more sustained baseflow from ~~the~~ Hol tributary, the
730 reduced extent of the primary aquifer results in a dominance in slow groundwater flow from
731 this tributary. Similarly, ~~the~~ Kruismans is dominated by shale formations which result in a

732 larger interflow contribution, although due to the limited baseflow contribution (37 %) the
733 streamflow from this tributary is highly variable, which impacts on its susceptibility to drought.

734 The results from this study have shown that while ~~the~~-Krom Antonies was initially believed to
735 be the major flow contributor, ~~the~~-Bergvallei is in fact the most significant, although
736 streamflow from the four tributaries is highly variable, with baseflow from ~~the~~-Hol tributary
737 the only constant input source. The presence of conductive TMG sandstones and quaternary
738 sediments in both ~~the~~-Krom Antonies and Bergvallei, results in quick baseflow responses with
739 little flow attenuation. The potential implication of a constant source of groundwater being
740 provided from ~~the~~-Hol tributary, is that if the groundwater is of poor quality this would result
741 in a constant input of saline groundwater, with ~~the~~-Krom Antonies and Bergvallei providing
742 freshwater only after sufficient rainfall has been received.

743 **5.3 Baseflow comparison**

744 The groundwater components of the J2000 model were adjusted using aquifer hydraulic
745 conductivity from a MODFLOW model of one of the main feeding tributaries of the
746 Verlorenvlei. ~~The~~-Krom Antonies was selected as it was previously believed to be the largest
747 input of groundwater to Verlorenvlei (Fig. 2). Baseflow for ~~the~~-Krom Antonies tributary was
748 previously calculated using a MODFLOW model (Watson, 2018), by considering aquifer
749 hydraulic conductivity and average groundwater recharge. As average recharge was used,
750 baseflow estimates from MODFLOW are likely to fall on the upper end of daily baseflow
751 values estimated by the J2000 model. For ~~the~~-Krom Antonies sub-catchment, Watson, (2018)
752 estimated baseflow between 14,000 to 19,000 $m^3.d^{-1}$ for 2010-2016 using MODFLOW. Similar
753 daily baseflow estimates from the J2000 were only exceeded 10 % of the time, with average
754 estimates (50 %) of 1,036 $m^3.d^{-1}$ over the course of the modelling period (Fig. 9).

755 The MODFLOW estimates were applied over the course of a wet cycle (2016). In comparison
756 to the MODFLOW estimates (14,000 to 19,000 $\text{m}^3.\text{d}^{-1}$) average baseflow from J2000 for 2016
757 was 8,214 $\text{m}^3.\text{d}^{-1}$. The daily timestep nature of the J2000 is likely to result in far lower baseflow
758 estimates, as recharge is only received over a 6-month period as opposed to a yearly average
759 estimate. One possible implication of this is that while common groundwater abstraction
760 scenarios have been based on yearly recharge, abstraction is likely to exceed sustainable
761 volumes during dry months or dry cycles and this could hinder the ability of the aquifer to
762 supply baseflow. While the groundwater components of the J2000 have been distributed to
763 allow for improved baseflow estimates, the groundwater calibration was applied to the Krom
764 Antonies. However, this study showed that Bergvallei has been identified as the largest water
765 contributor. In hindsight, the use of geochemistry to identify dominant tributaries could have
766 aided the groundwater model adaption. While it would have been beneficial to adapt the
767 groundwater components of the J2000 using the dominant baseflow contributor, considering
768 the geological heterogeneity between tributaries is more important for identifying how to adapt
769 the groundwater components of the J2000. While the distribution of aquifer components
770 improved modelled baseflow, including groundwater abstraction scenarios in baseflow
771 modelling in the sub-catchment is important for future water management for this ecologically
772 significant area.

773 **5.4 The Verlorenvlei reserve and the evaporative demand**

774 For this study, exceedance probabilities were estimated through rainfall/runoff modelling for
775 the previous 30-31 years within the Verlorenvlei sub-catchment. The exceedance probabilities
776 were determined for each tributary, as well as the total inflows into the lake. These exceedance
777 probabilities were compared with the evaporative demand of the lake, to understand whether
778 inflows are in surplus or whether the evaporation demand exceeds inflow.

779 From the exceedance probabilities generated in this study, the lake is predominately fed by less
780 frequent large discharge events, where on average the daily inflows to the lake do not sustain
781 the lake water level. This is particularly evident in the measured water level data from station
782 G3T001, where measured water levels have a large daily standard deviation (0.62) (Watson *et*
783 *al.*, 2018). [The daily inflows of water into the Verlorenvlei has also been subject to significant](#)
784 [rainfall variability, with yearly rainfall between the second wet cycle \(2007-2017\) being twice](#)
785 [as variable in comparison to the first wet cycle \(1987-1996\). The change in rainfall variability](#)
786 [has had a significant impact on soil moisture conditions, resulting in not only larger peak](#)
787 [discharges but also lengthened low flow conditions.](#) With climate change likely to impact the
788 length and severity of dry cycles, it is likely that the lake will dry up more frequently into the
789 future, which could have severe implications on the biodiversity that relies on the lake's habitat
790 for survival. Of importance to the lake's survival is the protection of river inflows during wet
791 cycles, where the lake requires these inflows for regeneration.

792 While the impact of irrigation could not be incorporated, over allocation of water resources
793 may potentially have a significant impact on the catchment water balance, especially during
794 wet cycles when ecosystems are recovering from dry conditions. The increased irrigation
795 during wet cycles as a result of agricultural development, could be a further impact on the
796 recovery of sensitive ecosystems. This type of issue is not limited to Verlorenvlei but applies
797 to many wetlands or estuarine lakes around the world, while they have been classified as
798 protected areas, water resources within the catchments are required for food security. As
799 climate change drives increased temperatures and variability in rainfall, the ± 10 -year cycles
800 of dry and wet conditions may no longer be valid anymore, where these conditions may shorten
801 or lengthen. With the routine breaking of weather records across the world (Bruce, 2018; Davis,
802 2018), it is becoming increasingly evident that conditions are changing and becoming more

803 variable, which could impact sensitive ecosystems around the world, highlighting the need for
804 effective water management protocols during times of limited rainfall.

805

806 **6. Conclusion**

807 Understanding river flow regime dynamics is important for the management of ecosystems that
808 are sensitive to streamflow fluctuations. While climatic factors impact rainfall volume~~s~~ during
809 wet and dry cycles, factors that control catchment runoff and baseflow are key to the
810 implementation of river protection strategies. In this study, groundwater components within
811 the J2000 model were distributed to improve baseflow and runoff proportioning for the
812 Verlorenvlei sub-catchment. The J2000 was distributed using groundwater model values for
813 the dominant baseflow tributary, while calibration was applied to the dominant streamflow
814 tributary. The model calibration was hindered by the DT limit, which reduced the confidence
815 in modelling high flow events, although an EMD filtering protocol was applied to account for
816 the resolution limitations and missing streamflow records. The modelling approach would
817 likely be transferable to other partially gauged semi-arid catchments, provided that
818 groundwater recharge is well constrained. The daily timestep nature of the J2000 model
819 allowed for an in-depth understanding of tributary flow regime dynamics, showing that while
820 streamflow variability is influenced by the runoff to baseflow proportion, the host rock or
821 sediment in which groundwater is held is also a factor that must be considered. The modelling
822 results showed that on average the streamflow influxes were not able to meet the evaporation
823 demand of the lake, with yearly rainfall becoming more variable. High-flow events, although
824 they occur infrequently, are responsible for regeneration of the lake's water level and ecology,
825 which illustrates the importance of wet cycles in maintaining biodiversity levels in semi-arid
826 environments. With climate change likely to impact the length and occurrence of dry cycle
827 conditions, wet cycles become particularly important for ecosystem regeneration, especially
828 for semi-arid regions such as the Verlorenvlei.

829 **7. Acknowledgements**

830 The authors would like to thank the WRC and SASSCAL for project funding as well as the
831 NRF and Iphakade for bursary support. Agricultural Research Council (ARC) and South
832 African Weather Service (SAWS) for their access to climate and rainfall data. The research
833 was carried out in the framework of SASSCAL and was funded by the German Federal
834 Ministry of Education and Research (BMBF) under promotion number 01LG1201E.

835 **8. References**

836 Acreman, M. C. and Dunbar, M. J.: Defining environmental river flow requirements – a review,
837 *Hydrol. Earth Syst. Sci.*, 8(5), 861–876, 2004.

838 Arnold, J. G., Srinivasan, R., Muttiah, R. S. and Williams, J. R.: Large area hydrologic
839 modeling and assessment Part I: Model development, , 34(1), 73–89, 1998.

840 Arthington, A. H., Kennen, J. G., Stein, E. D. and Webb, J. A.: Recent advances in
841 environmental flows science and water management — Innovation in the Anthropocene,
842 *Freshw. Biol.*, (March), 1–13, 2018.

843 Barker, I. and Kirmond, A.: Managing surface water abstraction in Wheater, H. and Kirby,
844 C.(eds) *Hydrology in a changing environment*, vol1, Br. Hydrol. Soc., 249–258, 1998.

845 Batjes, N., Dijkshoorn, K., Van Engelen, V., Fischer, G., Jones, A., Montanarella, L., Petri,
846 M., Prieler, S., Teixeira, E. and Wiberg, D.: Harmonized World Soil Database (version 1.2),
847 Tech. rep., FAO and IIASA, Rome, Italy and Laxenburg, Austria., 2012.

848 Bauer, P., Held, R. J., Zimmermann, S., Linn, F. and Kinzelbach, W.: Coupled flow and salinity
849 transport modelling in semi-arid environments: The Shashe River Valley, Botswana, J.
850 *Hydrol.*, 316(1–4), 163–183, 2006.

851 Bragg, O. M., Black, A. R., Duck, R. W. and Rowan, J. S.: Progress in Physical Geography
852 Approaching the physical-biological interface in rivers : a review of methods, , 4(October
853 2000), 506–531, 2005.

854 Bruce, D.: Prepare for extended severe weather seasons, Aust. J. Emerg. Manag., 33(4), 6,
855 2018.

856 Bunn, S. E. and Arthington, A. H.: Basic principles and ecological consequences of altered
857 flow regimes for aquatic biodiversity, Environ. Manage., 30(4), 492–507, 2002.

858 Conrad, J., Nel, J. and Wentzel, J.: The challenges and implications of assessing groundwater
859 recharge: A case study-northern Sandveld , Western Cape, South Africa, Water SA, 30(5), 75–
860 81, 2004.

861 Costanza, R., Arge, R., Groot, R. De, Farberk, S., Grasso, M., Hannon, B., Limburg, K.,
862 Naeem, S., O'Neill, R. V, Paruelo, J., Raskin, R. G., Suttonkk, P. and van den Belt, M.: The
863 value of the world's ecosystem services and natural capital, Nature, 387, 253–260, 1997.

864 CSIR: Development of the Verlorenvlei estuarine management plan: Situation assessment.
865 Report prepared for the C.A.P.E. Estuaries Programme, , 142, 2009.

866 Davis, G.: The Energy-Water-Climate Nexus and Its Impact on Queensland's Intensive
867 Farming Sector, in The Impact of Climate Change on Our Life, pp. 97–126, Springer., 2018.

868 Deb, K., Pratap, A., Agarwal, S. and Meyarivan, T.: A fast and elitist multiobjective genetic
869 algorithm: NSGA-II, IEEE Trans. Evol. Comput., 6(2), 182–197, 2002.

870 Diersch, H.-J. G.: FEFLOW reference manual, Inst. Water Resour. Plan. Syst. Res. Ltd, 278,
871 2002.

872 Domenico, P. A. and Schwartz, F. W.: Physical and Chemical Hydrogeology, John Wiley and

873 Sons, Inc., New York., 1990.

874 DWAF: Sandveld Preliminary (Rapid) Reserve Determinations. Langvlei, Jakkals and
875 Verlorenvlei Rivers. Olifants-Doorn WMA G30. Surface Volume 1: Final Report Reserve
876 Specifications. DWAF Project Number: 2002-227., 2003.

877 Flügel, W.: Delineating hydrological response units by geographical information system
878 analyses for regional hydrological modelling using PRMS/MMS in the drainage basin of the
879 River Bröl, Germany, *Hydrol. Process.*, 9(3-4), 423–436, 1995.

880 Gleeson, T. and Richter, B.: How much groundwater can we pump and protect environmental
881 flows through time? Presumptive standards for conjunctive management of aquifers and rivers,
882 *River Res. Appl.*, 34, 83–92, doi:10.1002/rra.3185, 2018.

883 Gleick, P. H.: Global freshwater resources: soft-path solutions for the 21st century, *Science*
884 (80- .), 302(5650), 1524–1528, 2003.

885 Harbaugh, Arlen, W.: MODFLOW-2005 , The U . S . Geological Survey Modular Ground-
886 Water Model — the Ground-Water Flow Process, *U.S. Geol. Surv. Tech. Methods*, 253, 2005.

887 Harbaugh, B. A. W., Banta, E. R., Hill, M. C. and Mcdonald, M. G.: MODFLOW-2000 , THE
888 U . S . GEOLOGICAL SURVEY MODULAR GROUND-WATER MODEL — USER
889 GUIDE TO MODULARIZATION CONCEPTS AND THE GROUND-WATER FLOW
890 PROCESS, Reston, Virginia., 2000.

891 Harman, C. and Stewardson, M.: Optimizing dam release rules to meet environmental flow
892 targets, *River Res. Appl.*, 21(2–3), 113–129, 2005.

893 Helme, N.: Botanical report: Fine Scale vegetation mapping in the Sandveld, as part of the
894 C.A.P.E programme., 2007.

895 Huang, N. E., Shen, Z., Long, S. R., Wu, M. C., Shih, H. H., Zheng, Q., Yen, N.-C., Tung, C.
896 C. and Liu, H. H.: The empirical mode decomposition and the Hilbert spectrum for nonlinear
897 and non-stationary time series analysis, in Proceedings of the Royal Society of London A:
898 mathematical, physical and engineering sciences, vol. 454, pp. 903–995, The Royal Society.,
899 1998.

900 Huang, Y., Schmitt, F. G., Lu, Z. and Liu, Y.: Analysis of daily river flow fluctuations using
901 empirical mode decomposition and arbitrary order Hilbert spectral analysis, *J. Hydrol.*, 373(1–
902 2), 103–111, 2009.

903 Hughes, D. A.: Providing hydrological information and data analysis tools for the
904 determination of ecological instream flow requirements for South African rivers, *J. Hydrol.*,
905 241(1–2), 140–151, 2001.

906 Hughes, D. A. and Hannart, P.: A desktop model used to provide an initial estimate of the
907 ecological instream flow requirements of rivers in South Africa, *J. Hydrol.*, 270(3–4), 167–
908 181, 2003.

909 Jenson, S. K. and Domingue, J. O.: Extracting topographic structure from digital elevation data
910 for geographic information system analysis, *Photogramm. Eng. Remote Sensing*, 54(11),
911 1593–1600, 1988.

912 Johnson, M. R., Anhaeuesser, C. R. and Thomas, R. J.: The Geology of South Africa, Geological
913 Society of South Africa., 2006.

914 Kim, N. W., Chung, I. M., Won, Y. S. and Arnold, J. G.: Development and application of the
915 integrated SWAT-MODFLOW model, *J. Hydrol.*, 356(1–2), 1–16, 2008.

916 King, J. and Louw, D.: Instream flow assessments for regulated rivers in South Africa using
917 the Building Block Methodology, *Aquat. Ecosyst. Health Manag.*, 1(2), 109–124, 1998.

918 Kisi, O., Latifoğlu, L. and Latifoğlu, F.: Investigation of empirical mode decomposition in
919 forecasting of hydrological time series, *Water Resour. Manag.*, 28(12), 4045–4057, 2014.

920 Krause, P.: Das hydrologische Modellsystem J2000. Beschreibung und Anwendung in großen
921 Flussgebieten, in *Umwelt/Environment*, Vol. 29. Jülich: Research centre., 2001.

922 Krause, P., Boyle, D. P. and Bäse, F.: Comparison of different efficiency criteria for
923 hydrological model assessment, *Adv. Geosci.*, 5, 89–97, 2005.

924 Leavesley, G. H. and Stannard, L. G.: Application of remotely sensed data in a distributed-
925 parameter watershed model, in *Proceedings of the Workshop on Applications of Remote
926 Sensing in Hydrology*, Saskatoon, pp. 47–64., 1990.

927 Lynch, S.: Development of a raster database of annual, monthly and daily rainfall for southern
928 Africa, Pietermaritzburg., 2004.

929 Martens, K., Davies, B. R., Baxter, A. J. and Meadows, M. E.: A contribution to the taxonomy
930 and ecology of the Ostracoda (Crustacea) from Verlorenvlei (Western Cape, South Africa),
931 *African Zool.*, 31(1), 22–36, 1996.

932 Meinhardt, M., Fleischer, M., Fink, M., Kralisch, S., Kenabatho, P., de Clercq, W. P., Zimba,
933 H., Phiri, W. and Helmschrot, J.: Semi-arid catchments under change: Adapted hydrological
934 models to simulate the influence of climate change and human activities on rainfall-runoff
935 processes in southern Africa, in *Climate change and adaptive land management in southern
936 Africa – assessments, changes, challenges, and solutions*, edited by N. Revermann, R.,
937 Krewenka, K.M., Schmiedel, U., Olwoch, J.M., Helmschrot, J. & Jürgens, pp. 114–130, Klaus
938 Hess Publishers, Göttingen & Windhoek., 2018.

939 Miller, J. A., Dunford, A. J., Swana, K. A., Palcsu, L., Butler, M. and Clarke, C. E.: Stable
940 isotope and noble gas constraints on the source and residence time of spring water from the

941 Table Mountain Group Aquifer, Paarl, South Africa and implications for large scale
942 abstraction, *J. Hydrol.*, 551, 100–115, 2017.

943 Muche, G., Kruger, S., Hillman, T., Josenhans, K., Ribeiro, C., Bazibi, M., Seely, M., Nkonde,
944 E., de Clercq, W. P., Strohbach, B., Kenabatho, K. ., Vogt, R., Kaspar, F., Helmschrot, J. and
945 Jürgens, N.: Climate change and adaptive land management in southern Africa – assessments,
946 changes, challenges, and solutions, in *Biodiversity & Ecology*, edited by R. Revermann, K. M.
947 Krewenka, U. Schmiedel, J. . Olwoch, J. Helmschrot, and N. Jürgens, pp. 34–43, Klaus Hess
948 Publishers, Göttingen & Windhoek., 2018.

949 Nelson, E., Mendoza, G., Regetz, J., Polasky, S., Tallis, H., Cameron, Dr., Chan, K. M. A.,
950 Daily, G. C., Goldstein, J. and Kareiva, P. M.: Modeling multiple ecosystem services,
951 biodiversity conservation, commodity production, and tradeoffs at landscape scales, *Front.*
952 *Ecol. Environ.*, 7(1), 4–11, 2009.

953 O’Keeffe, J.: Sustaining river ecosystems: Balancing use and protection, *Prog. Phys. Geogr.*,
954 33(3), 339–357, 2009.

955 Olden, J. D. and Naiman, R. J.: Incorporating thermal regimes into environmental flows
956 assessments: Modifying dam operations to restore freshwater ecosystem integrity, *Freshw.*
957 *Biol.*, 55(1), 86–107, 2010.

958 Pfannschmidt, K.: Optimierungsmethoden zur HRU-basierten N/A-Modellierung für eine
959 operationelle Hochwasservorhersage auf Basis prognostischer Klimadaten des Deutschen
960 Wetterdienstes: Untersuchungen in einem mesoskaligen Einzugsgebiet im Thüringer Wald,
961 2008.

962 Pfennig, B., Kipka, H., Fink, M., Wolf, M., Krause, P. and Flügel, W.-A.: Development of an
963 extended routing scheme in reference to consideration of multi-dimensional flow relations

964 between hydrological model entities, 18th World IMACS / MODSIM Congr. Cairns, Aust. 13-
965 17 July 2009., 2009.

966 Poff, N. L., Allan, J. D., Bain, M. B., Karr, J. R., Prestegaard, K. L., Richter, B. D., Sparks, R.
967 E. and Stromberg, J. C.: A paradigm for river conservation and restoration, *Bioscience*, 47(11),
968 769–784, 1997.

969 Poff, N. L., Richter, B. D., Arthington, A. H., Bunn, S. E., Naiman, R. J., Kendy, E., Acreman,
970 M., Apse, C., Bledsoe, B. P., Freeman, M. C., Henriksen, J., Jacobson, R. B., Kennen, J. G.,
971 Merritt, D. M., O’Keeffe, J. H., Olden, J. D., Rogers, K., Tharme, R. E. and Warner, A.: The
972 ecological limits of hydrologic alteration (ELOHA): A new framework for developing regional
973 environmental flow standards, *Freshw. Biol.*, 55(1), 147–170, 2010.

974 Postel, S. and Carpenter, S.: Freshwater ecosystem services, *Nature’s Serv. Soc. Depend. Nat.*
975 *Ecosyst.*, 195, 1997.

976 Postel, S. and Richter, B.: Rivers for life: managing water for people and nature, Island Press.,
977 2012.

978 Richter, B. D.: Re-thinking environmental flows: from allocations and reserves to sustainability
979 boundaries, *River Res. Appl.*, 26(8), 1052–1063, 2010.

980 Richter, B. D., Mathews, R., Harrison, D. L. and Wigington, R.: Ecologically sustainable water
981 management: Managing river flows for ecological integrity, *Ecol. Appl.*, 13(1), 206–224, 2003.

982 Richter, B. D., Davis, M. M., Apse, C. and Konrad, C.: A presumptive standard for
983 environmental flow protection, *River Res. Appl.*, 28, 1312–1321, 2012.

984 Ridoutt, B. G. and Pfister, S.: A revised approach to water footprinting to make transparent the
985 impacts of consumption and production on global freshwater scarcity, *Glob. Environ. Chang.*,

986 20(1), 113–120, 2010.

987 Rozendaal, A. and Gresse, P. G.: Structural setting of the Riviera W-Mo deposit, western Cape,
988 South Africa, *South African J. Geol.*, 97(2), 184, 1994.

989 Sigidi, N. T.: Geochemical and isotopic tracing of salinity loads into the Ramsar listed
990 Verlorenvlei freshwater estuarine lake , Western Cape , South Africa, (Unpublished MSc
991 thesis) Stellenbosch University., 2018.

992 Sinclair, S., Lane, S. and Grindley, J.: Estuaries of the Cape: Part II: Synopses of avaialble
993 information on individual systems., Stellenbosch., 1986.

994 SRK: Preliminary Assessment of Impact of the Proposed Riviera Tungsten Mine on
995 Groundwater Resources Preliminary Assessment of Impact of the Proposed Riviera Tungsten
996 Mine on Groundwater Resources., 2009.

997 Steudel, T., Bugan, R., Kipka, H., Pfennig, B., Fink, M., de Clercq, W., Flügel, W.-A. and
998 Helmschrot, J.: Implementing contour bank farming practices into the J2000 model to improve
999 hydrological and erosion modelling in semi-arid Western Cape Province of South Africa,
1000 *Hydrol. Res.*, 46(2), 192, 2015.

1001 Tennant, D. L.: Instream Flow Regimens for Fish , Wildlife , Recreation and Related
1002 Environmental Resources, *Fisheries*, 1(4), 6–10, 1976.

1003 UMVOTO-SRK: Reconnaissance investigation into the development and utilization of the
1004 Table Mountain Group Artesian Groundwater, using the E10 catchment as a pilot study area.,
1005 2000.

1006 Vetger, J. R.: An explanation of a set of national groundwater maps. WRC report TT 74/95,
1007 Water Res. Comm. Pretoria, South Africa, 1995.

1008 Wagener, T. and Wheater, H. S.: Parameter estimation and regionalization for continuous
1009 rainfall-runoff models including uncertainty, *J. Hydrol.*, 320(1–2), 132–154, 2006.

1010 Watson, A. P.: Using distributive surface water and groundwater modelling techniques to
1011 quantify groundwater recharge and baseflow for the Verlorenvlei estuarine system , west coast
1012 , South Africa, (Unpublished PhD thesis) Stellenbosch University., 2018.

1013 Watson, A. P., Miller, J. A., Fleischer, M. and de Clercq, W. P.: Estimation of groundwater
1014 recharge via percolation outputs from a rainfall/runoff model for the Verlorenvlei estuarine
1015 system, west coast, South Africa., *J. Hydrol.*, 558(C), 238–254, 2018.

1016 Weaver, J. and Talma, A.: Cumulative rainfall collectors – A tool for assessing groundwater
1017 recharge, , 31(3), 283–290, 2005.

1018 Willems, P.: A time series tool to support the multi-criteria performance evaluation of rainfall-
1019 runoff models, *Environ. Model. Softw.*, 24(3), 311–321, doi:10.1016/j.envsoft.2008.09.005,
1020 2009.

1021 Wishart, M. J.: The terrestrial invertebrate fauna of a temporary stream in southern Africa,
1022 *African Zool.*, 35(2), 193–200, 2000.

1023 Wu, Y.: Groundwater recharge estimation in Table Mountain Group aquifer systems with a
1024 case study of Kammanassie area, 2005.

1025 Young, A. R.: Stream flow simulation within UK ungauged catchments using a daily rainfall-
1026 runoff model, *J. Hydrol.*, 320, 155–172, 2006.

1027